# High statistics analysis using anisotropic clover lattices: IV. Volume dependence of light hadron masses

S. R. Beane, E. Chang, W. Detmold, H. W. Lin, T. C. Luu, K. Orginos, A. Parreño, M. J. Savage, A. Torok, and A. Walker-Loud (NPLQCD Collaboration)

Phys. Rev. D **84**, 014507 — Published 25 July 2011

DOI: 10.1103/PhysRevD.84.014507

# High Statistics Analysis using Anisotropic Clover Lattices: (IV) Volume Dependence of Light Hadron Masses

S.R. Beane,[1,2] E. Chang,[3] W. Detmold,[4,5] H.W. Lin,[6] T.C. Luu,[7]
K. Orginos,[4,5] A. Parreño,[3] M.J. Savage,[6] A. Torok,[8] and A. Walker-Loud[9]

(NPLQCD Collaboration)

[1]*Albert Einstein Zentrum für Fundamentale Physik, Institut für Theoretische Physik, Sidlerstrasse 5, CH-3012 Bern, Switzerland*
[2]*Department of Physics, University of New Hampshire, Durham, NH 03824-3568, USA*
[3]*Dept. d'Estructura i Constituents de la Matèria. Institut de Ciències del Cosmos (ICC), Universitat de Barcelona, Martí Franquès 1, E08028-Spain*
[4]*Department of Physics, College of William and Mary, Williamsburg, VA 23187-8795, USA*
[5]*Jefferson Laboratory, 12000 Jefferson Avenue, Newport News, VA 23606, USA*
[6]*Department of Physics, University of Washington, Box 351560, Seattle, WA 98195, USA*
[7]*N Division, Lawrence Livermore National Laboratory, Livermore, CA 94551, USA*
[8]*Department of Physics, Indiana University, Bloomington, IN 47405, USA*
[9]*Lawrence Berkeley National Laboratory, Berkeley, CA 94720, USA*

(Dated: July 5, 2011 - 13:12)

## Abstract

The volume dependence of the octet baryon masses and relations among them are explored with Lattice QCD. Calculations are performed with $n_f = 2 + 1$ clover fermion discretization in four lattice volumes, with spatial extent $L \sim 2.0, 2.5, 3.0$ and 3.9 fm, with an anisotropic lattice spacing of $b_s \sim 0.123$ fm in the spatial direction, and $b_t = b_s/3.5$ in the time direction, and at a pion mass of $m_\pi \sim 390$ MeV. The typical precision of the ground-state baryon mass determination is $\lesssim 0.2\%$, enabling a precise exploration of the volume dependence of the masses, the Gell-Mann–Okubo mass relation, and of other mass combinations. A comparison of the volume dependence with the predictions of heavy baryon chiral perturbation theory is performed in both the $\mathrm{SU}(2)_L \otimes \mathrm{SU}(2)_R$ and $\mathrm{SU}(3)_L \otimes \mathrm{SU}(3)_R$ expansions. Predictions of the three-flavor expansion for the hadron masses are found to describe the observed volume dependences reasonably well. Further, the $\Delta N\pi$ axial coupling constant is extracted from the volume dependence of the nucleon mass in the two-flavor expansion, with only small modifications in the three-flavor expansion from the inclusion of kaons and $\eta$'s. At a given value of $m_\pi L$, the finite-volume contributions to the nucleon mass are predicted to be significantly smaller at $m_\pi \sim 140$ MeV than at $m_\pi \sim 390$ MeV due to a coefficient that scales as $\sim m_\pi^3$. This is relevant for the design of future ensembles of lattice gauge-field configurations. Finally, the volume dependence of the pion and kaon masses are analyzed with two-flavor and three-flavor chiral perturbation theory.

## I. INTRODUCTION

The calculation of the properties and interactions of light nuclei is a major goal of Lattice QCD. While Lattice QCD calculations at the physical light-quark masses, including strong isospin breaking and electroweak interactions, are a number of years in the future, precision calculations of hadron masses are being performed today in the isospin limit and without electroweak interactions over a range of light-quark masses. The masses of the baryons and nuclei are in the GeV energy regime, but the typical excitation energies and binding energies found in light nuclei are in the MeV energy regime. This hierarchy presents a significant challenge for Lattice QCD calculations as correlation functions must be determined with exceptionally high precision in order to obtain statistically significant energy differences that yield nuclear excitation and binding energies.

A source of systematic uncertainty in the extraction of scattering parameters and nuclear binding energies is the volume dependence of the hadron masses themselves. Given that the deuteron binding energy is $B_D \sim 2.2$ MeV, an accurate Lattice QCD calculation of this energy will require that the nucleon mass be known to a precision of $\Delta M_N \ll 1$ MeV. This includes the contribution from the finite lattice volume. Further, the exponential volume corrections to Lüscher's eigenvalue relation [1–3] are also required to be small [4, 5]. In our recent calculation of the H-dibaryon binding energy [6], the volume dependence of the $\Lambda$-baryon mass was presented, and it was concluded that the standard rule-of-thumb, $m_\pi L \gtrsim 2\pi$, is in fact necessary at a pion mass of $m_\pi \sim 390$ MeV in order for the $\Lambda$ finite-volume mass shift to be much smaller than the observed binding energy.

In this work, which is a continuation of our high statistics Lattice QCD explorations [7–9], we present results for the volume dependence of the masses of the baryons in the lowest-lying SU(3)-flavor octet, and of relations among them, calculated with four ensembles of $n_f = 2 + 1$ anisotropic clover gauge-field configurations at a pion mass of $m_\pi \sim 390$ MeV with a spatial lattice spacing of $b_s \sim 0.123$ fm, an anisotropy of $\xi = 3.5$ and with cubic volumes of spatial extent $L \sim 2.0, 2.5, 3.0$ and 3.9 fm. The volume dependence of the pion and kaon masses are also determined. Having the multiple lattice volumes with all of the other parameters fixed is critical to fully understanding the volume dependence of the hadron masses and other quantities. In particular, lattice-spacing artifacts, which enter at $\mathcal{O}(b_s^2)$, are the same in all four ensembles to very high precision. The results of the Lattice QCD calculations are compared with the expectations from next-to-leading-order (NLO) chiral perturbation theory ($\chi$PT) and heavy-baryon chiral perturbation theory (HB$\chi$PT) with two and three flavors of active quarks [1]. While it is interesting to compare the calculated volume dependences with the corresponding expectations from low-energy effective field theories (EFT), perhaps the most important reason for such a study is in order to plan for the future production of ensembles of lattice gauge-field configurations. An interesting result of this study is that while the octet baryons experience significant and quantifiable finite-volume corrections, the pion and the kaon, whose masses are determined at the 0.1% level, show effectively no finite-volume effects. That is, the pions and kaons are in the infinite-volume regime for the pion mass and the range of volumes that we explore. These results are consistent with the expectations derived from $\chi$PT and HB$\chi$PT.

[1] The leading volume dependence of the hadron masses arises at NLO in the chiral expansion. The leading order (LO) contributions to hadron masses from local operators make vanishing contributions to the volume dependence.

The first realistic attempt to determine the coefficients of counterterms in the chiral Lagrangian from the volume dependence of the nucleon mass was performed in Ref. [10]. The coefficients in the $\mathrm{SU}(2)_L \otimes \mathrm{SU}(2)_R$ chiral Lagrangian without dynamical $\Delta$'s were constrained by the results of $n_f = 2$ Lattice QCD calculations using the clover discretization with $m_\pi \gtrsim 550$ MeV and with lattices of spatial extent $L \lesssim 2.2$ fm. The precision of these calculations was substantially lower than in the present work, nonetheless, nontrivial constraints were found on the values of coefficients in the chiral Lagrangian at NNLO in the expansion by using phenomenologically determined values for the NLO constants. These constraints should be viewed only as a demonstration of the method, given the large pion masses.

This paper is organized as follows. In section II, we formulate finite-volume correction formulas for octet-baryon masses to NLO in $\mathrm{SU}(2)_L \otimes \mathrm{SU}(2)_R$ and $\mathrm{SU}(3)_L \otimes \mathrm{SU}(3)_R$ HB$\chi$PT. Section III gives a concise description of the specific Lattice QCD calculations that are used in the present finite-volume study. In section IV, we analyze the octet-baryon finite-volume effects, first (in subsection IV A) using a simple, intuitive description, and then (in subsection IV B) using HB$\chi$PT. In subsection IV C, various combinations of baryon masses are likewise analyzed. In section V, we consider the finite-volume dependence of the pion and kaon masses and in section VI we conclude.

## II. FINITE-VOLUME CHIRAL PERTURBATION THEORY

### A. The Nucleon in $\mathrm{SU}(2)_L \otimes \mathrm{SU}(2)_R$ HB$\chi$PT

As the Goldstone bosons are the lightest hadrons, $\chi$PT is the appropriate tool to develop systematic expansions to describe finite-volume effects [11–13]. The crucial observation is that if the hadronic system is in a sufficiently large volume, then the infinite-volume chiral Lagrangian can be used to calculate finite-volume corrections, with no further operators required [2]. At NLO in HB$\chi$PT, the finite-volume corrections to the nucleon mass arise from one-loop self-energy diagrams with nucleon and $\Delta$ intermediate states and, in the limit of

[2] The finite-volume corrections are related to forward scattering amplitudes [14–16]. For instance [15],

$$M_N(m_\pi, L) - M_N(m_\pi, \infty) \;=\; M_N \; \frac{3\varepsilon_\pi^2}{4\pi^2} \sum_{\mathbf{n}\neq\mathbf{0}} \frac{1}{|\mathbf{n}| m_\pi L} \; \Big[ \; 2\pi \varepsilon_\pi g_{\pi N}^2 e^{-|\mathbf{n}| m_\pi L \, \sqrt{1-\varepsilon_\pi^2}} - \int_{-\infty}^{\infty} dy \; \tilde{D}^+(y) \; e^{-|\mathbf{n}| m_\pi L \, \sqrt{1+y^2}} \; \Big] \; + \; \mathcal{O}(e^{-\overline{M} L}) \quad , \tag{1}$$

where $\varepsilon_\pi = m_\pi/(2M_N)$, $\overline{M} \geq \sqrt{3/2} m_\pi$ and $\tilde{D}^+(y) = M_N \; D^+(i m_\pi y, 0)$, which is related to forward $\pi N$ scattering via

$$T(\pi^a(q) + N(p) \to \pi^{a'}(q') + N(p')) \;=\; \delta_{aa'} T^+ \; + \; \frac{1}{2} \left[\tau_{a'}, \tau_a\right] \; T^-$$
$$T^\pm \;=\; \overline{u'} \Big[ \; D^\pm(\nu, t) \; - \; \frac{1}{4M_N} \left[\not{q}, \not{q}\right] \; B^\pm(\nu, t) \; \Big] u \quad . \tag{2}$$

The strong coupling between the nucleon and pion is $g_{\pi N}$, which is related to the axial coupling constant via the chiral expansion $g_{\pi N} = g_A M_N \sqrt{2}/f_\pi + ...$ where $f_\pi \sim 132$ MeV. Evaluating eq. (1) at NLO in HB$\chi$PT recovers the perturbative result of eq. (3).

exact isospin symmetry, are given by [10, 17] [3]

$$\begin{aligned}\delta M_N &= M_N(m_\pi, L) - M_N(m_\pi, \infty) \ ; \\ &= \frac{9 m_\pi^3 g_A^2}{8\pi f_\pi^2} \ F_N^{(FV)}(m_\pi L) \ + \ \frac{m_\pi^3 g_{\Delta N \pi}^2}{\pi f_\pi^2} \ F_\Delta^{(FV)}(m_\pi L, \Delta_{\Delta N} L) \ , \end{aligned} \tag{3}$$

where the loop functions are defined to be

$$F_N^{(FV)}(x) \ = \ \frac{1}{6} \sum_{\mathbf{n} \neq \mathbf{0}} \frac{e^{-|\mathbf{n}|x}}{|\mathbf{n}|x} \ = \ \frac{e^{-x}}{x} \ + \ 2 \ \frac{e^{-\sqrt{2}x}}{\sqrt{2}x} \ + \ \frac{4}{3} \ \frac{e^{-\sqrt{3}x}}{\sqrt{3}x} \ + \ ... \ ; \tag{4}$$

$$F_\Delta^{(FV)}(x,y) \ = \ \frac{1}{3\pi} \sum_{\mathbf{n} \neq \mathbf{0}} \int_0^\infty dw \ \overline{\beta}(w, \frac{y}{x}) \ \left[ \overline{\beta}(w, \frac{y}{x}) \ K_0 \left( |\mathbf{n}| x \overline{\beta}(w, \frac{y}{x}) \right) - \frac{K_1 \left( |\mathbf{n}| x \overline{\beta}(w, \frac{y}{x}) \right)}{|\mathbf{n}| x} \right] ; \tag{5}$$

where $\overline{\beta}(w,z) \ = \ \sqrt{w^2 + 2zw + 1}$, $\Delta_{\Delta N} = M_\Delta - M_N$, and the $K_n(z)$ are modified Bessel functions. In the limit $\Delta \to 0$, $F_\Delta^{(FV)}(m_\pi L, \Delta L) \to F_N^{(FV)}(m_\pi L)$. For asymptotically large lattice volumes, it is expected that only the leading contributions in the sums in eq. (4) and eq. (5) will be relevant.

### B. The Hyperons in $\mathrm{SU}(2)_L \otimes \mathrm{SU}(2)_R$ HB$\chi$PT

It is straightforward to compute the finite-volume corrections to the hyperon masses at NLO in $\mathrm{SU}(2)_L \otimes \mathrm{SU}(2)_R$ HB$\chi$PT. One finds, in a generalization of eq. (3), that

$$\delta M_\Lambda \ = \ \frac{3 \ g_{\Lambda\Sigma}^2 \ m_\pi^3}{8\pi f_\pi^2} F_\Delta^{(FV)}(m_\pi L, \Delta_{\Sigma\Lambda} L) \ + \ \frac{3 g_{\Sigma^*\Lambda\pi}^2 \ m_\pi^3}{2\pi f_\pi^2} F_\Delta^{(FV)}(m_\pi L, \Delta_{\Sigma^*\Lambda} L) \ ; \tag{6}$$

$$\begin{aligned}\delta M_\Sigma \ &= \ \frac{g_{\Lambda\Sigma}^2 \ m_\pi^3}{8\pi f_\pi^2} F_\Delta^{(FV)}(m_\pi L, \Delta_{\Lambda\Sigma} L) \ + \ \frac{3 g_{\Sigma\Sigma}^2 \ m_\pi^3}{4\pi f_\pi^2} F_N^{(FV)}(m_\pi L) \\ &\qquad + \ \frac{g_{\Sigma^*\Sigma\pi}^2 \ m_\pi^3}{2\pi f_\pi^2} F_\Delta^{(FV)}(m_\pi L, \Delta_{\Sigma^*\Sigma} L) \ ; \end{aligned} \tag{7}$$

$$\delta M_\Xi \ = \ \frac{9 g_{\Xi\Xi}^2 \ m_\pi^3}{8\pi f_\pi^2} F_N^{(FV)}(m_\pi L) \ + \ \frac{3 g_{\Xi^*\Xi\pi}^2 \ m_\pi^3}{4\pi f_\pi^2} F_\Delta^{(FV)}(m_\pi L, \Delta_{\Xi^*\Xi} L) \ , \tag{8}$$

where $\Delta_{AB} \equiv M_B - M_A$. For definitions of the various axial couplings in terms of chiral Lagrangian operators, see Ref. [18]. In this formulation of hyperon finite-volume effects, the contributions from kaon and $\eta$ loops are in the coefficients of local operators, and therefore do not contribute until higher orders in the chiral expansion (as the finite-volume effects arise from pion loops). This implies that for quark masses such that $m_\pi < m_K$ (but not $m_\pi \ll m_K$) there is a region where the two-flavor chiral expansion of infinite-volume quantities will converge but finite-volume effects will not be accounted for systematically in the two-flavor expansion.

---

[3] The substitutions $w \to \lambda/m_\pi$, $z \to \Delta/m_\pi$, $\overline{\beta}(w, \frac{y}{x}) \to \beta_\Delta/m_\pi$, $y \to \Delta L$, $x \to m_\pi L$, and $F_\Delta^{(FV)}(x,y) \to -\mathcal{K}(\Delta)/(3\pi m_\pi^3)$ recover the expressions given in Ref. [17].

### C. The Baryon Octet in $\mathrm{SU}(3)_L \otimes \mathrm{SU}(3)_R$ HB$\chi$PT

In addition to the contributions to the volume dependence from higher orders in the $\mathrm{SU}(2)_L \otimes \mathrm{SU}(2)_R$ chiral expansion, there are contributions from quantum fluctuations of the nucleon into strange hadrons, and of the hyperons into other members of the baryon octet. For instance, in addition to the $\pi N$ and $\pi\Delta$ intermediate states that give finite volume contributions to the nucleon mass, intermediate states such as $\Lambda K$ or $N\eta$ also contribute. Such fluctuations give rise to a volume dependence that scales as $\sim m_K^2\ e^{-m_K L}/L$ or $\sim m_\eta^2\ e^{-m_\eta L}/L$. In the Lattice calculations presented in this paper, $m_K/m_\pi \sim 1.4$, and as a result, such contributions are naively expected to be of the same magnitude as the $\sim m_\pi^2\ e^{-\sqrt{2}m_\pi L}/L$ contributions, which are suppressed compared with the leading volume dependence. As the axial-couplings between the nucleons and pions are of order one, and the couplings to strange intermediate states are generically small, such strange contributions are expected to be small. The explicit contributions to the octet-baryon mass shifts, written in terms of the SU(3)-symmetric axial couplings $D$, $F$ and $\mathcal{C}$ [19] are for the nucleon,

$$\begin{aligned}\delta M_N^{(K,\eta)} \;=\; & (D-F)^2\ \frac{9m_K^3}{8\pi f_K^2}\ F_\Delta^{(FV)}(m_K L, \Delta_{\Sigma N} L)\ +\ (D+3F)^2\ \frac{m_K^3}{8\pi f_K^2}\ F_\Delta^{(FV)}(m_K L, \Delta_{\Lambda N} L) \\ & +\ (D-3F)^2\ \frac{m_\eta^3}{8\pi f_\eta^2}\ F_\Delta^{(FV)}(m_\eta L, 0)\ +\ \mathcal{C}^2\ \frac{m_K^3}{4\pi f_K^2}\ F_\Delta^{(FV)}(m_K L, \Delta_{\Sigma^* N} L) \quad , \end{aligned} \tag{9}$$

and for the hyperons,

$$\begin{aligned}\delta M_\Lambda^{(K,\eta)} \;=\; & (D+3F)^2 \frac{m_K^3}{4\pi f_K^2}\ F_\Delta^{(FV)}(m_K L, \Delta_{N\Lambda} L)\ +\ (D-3F)^2 \frac{m_K^3}{4\pi f_K^2}\ F_\Delta^{(FV)}(m_K L, \Delta_{\Xi\Lambda} L) \\ & +\ D^2 \frac{m_\eta^3}{2\pi f_\eta^2}\ F_\Delta^{(FV)}(m_\eta L, 0)\ +\ \mathcal{C}^2 \frac{m_K^3}{2\pi f_K^2}\ F_\Delta^{(FV)}(m_K L, \Delta_{\Xi^*\Lambda} L) \quad , \end{aligned} \tag{10}$$

$$\begin{aligned}\delta M_\Sigma^{(K,\eta)} \;=\; & (D-F)^2 \frac{3m_K^3}{4\pi f_K^2}\ F_\Delta^{(FV)}(m_K L, \Delta_{N\Sigma} L)\ +\ (D+F)^2 \frac{3m_K^3}{4\pi f_K^2}\ F_\Delta^{(FV)}(m_K L, \Delta_{\Xi\Sigma} L) \\ & +\ D^2 \frac{m_\eta^3}{2\pi f_\eta^2}\ F_\Delta^{(FV)}(m_\eta L, 0)\ +\ \mathcal{C}^2 \frac{m_\eta^3}{4\pi f_\eta^2}\ F_\Delta^{(FV)}(m_\eta L, \Delta_{\Sigma^*\Sigma} L) \\ & +\ \mathcal{C}^2 \frac{2m_K^3}{3\pi f_K^2}\ F_\Delta^{(FV)}(m_K L, \Delta_{\Delta\Sigma} L)\ +\ \mathcal{C}^2 \frac{m_K^3}{6\pi f_K^2}\ F_\Delta^{(FV)}(m_K L, \Delta_{\Xi^*\Sigma} L) \quad , \end{aligned} \tag{11}$$

$$\begin{aligned}\delta M_\Xi^{(K,\eta)} \;=\; & (D+F)^2 \frac{9m_K^3}{8\pi f_K^2}\ F_\Delta^{(FV)}(m_K L, \Delta_{\Sigma\Xi} L)\ +\ (D-3F)^2 \frac{m_K^3}{8\pi f_K^2}\ F_\Delta^{(FV)}(m_K L, \Delta_{\Lambda\Xi} L) \\ & +\ (D+3F)^2 \frac{m_\eta^3}{8\pi f_\eta^2}\ F_\Delta^{(FV)}(m_\eta L, 0)\ +\ \mathcal{C}^2 \frac{m_\eta^3}{4\pi f_\eta^2}\ F_\Delta^{(FV)}(m_\eta L, \Delta_{\Xi^*\Xi} L) \\ & +\ \mathcal{C}^2 \frac{m_K^3}{4\pi f_K^2}\ F_\Delta^{(FV)}(m_K L, \Delta_{\Sigma^*\Xi} L)\ +\ \mathcal{C}^2 \frac{m_K^3}{2\pi f_K^2}\ F_\Delta^{(FV)}(m_K L, \Delta_{\Omega\Xi} L) \quad . \end{aligned} \tag{12}$$

In the limit of exact SU(3) symmetry, the SU(2) axial couplings introduced above are related to the SU(3) couplings via:

$$\begin{aligned} & g_A = D+F \quad , \quad g_{\Delta N\pi} = \mathcal{C} \quad , \quad g_{\Lambda\Sigma} = 2D \quad , \quad g_{\Sigma^*\Lambda\pi} = \mathcal{C}/\sqrt{2}\ , \\ & g_{\Sigma\Sigma} = 2F \quad , \quad g_{\Sigma^*\Sigma\pi} = \mathcal{C}/\sqrt{3} \quad , \quad g_{\Xi\Xi} = D-F \quad , \quad g_{\Xi^*\Xi\pi} = \mathcal{C}/\sqrt{3} \quad . \end{aligned} \tag{13}$$

Adding the finite-volume modifications in eqs. (9)-(12) to those in eq. (3) and eqs. (6)-(8) gives the full NLO $\mathrm{SU}(3)_L \otimes \mathrm{SU}(3)_R$ HB$\chi$PT finite-volume contributions to the baryons in the lowest-lying octet.

## III. DETAILS OF THE LATTICE QCD CALCULATION

Anisotropic gauge-field configurations have proven useful for the study of hadronic spectroscopy [20–23], and, as the calculations required for studying multi-hadron systems rely heavily on spectroscopy, we have put considerable effort into calculations using ensembles of gauge fields with clover-improved Wilson fermion actions with anisotropic lattice spacing that have been generated by the Hadron Spectrum Collaboration (HSC). In particular, the $n_f = 2 + 1$ flavor anisotropic clover Wilson action [24, 25] with stout-link smearing [26] of the spatial gauge fields in the fermion action with a smearing weight of $\rho = 0.14$ and $n_\rho = 2$ has been used. The gauge fields entering the fermion action are not smeared in the time direction, thus preserving the ultra-locality of the action in the time direction. Further, a tree-level tadpole-improved Symanzik gauge action without a $1 \times 2$ rectangle in the time direction is used.

The present calculations are performed on four ensembles of gauge-field configurations with $L^3 \times T$ of $16^3 \times 128$, $20^3 \times 128$, $24^3 \times 128$ and $32^3 \times 256$ lattice sites, with a renormalized anisotropy $\xi = b_s/b_t = 3.5$ where $b_s$ and $b_t$ are the spatial and temporal lattice spacings, respectively. The spatial lattice spacing of each ensemble is $b_s = 0.1227 \pm 0.0008$ fm [22] giving spatial lattice extents of $L \sim 2.0, 2.5, 3.0$ and 3.9 fm respectively. The same input light-quark mass parameters, $b_t m_l = -0.0840$ and $b_t m_s = -0.0743$, are used in the production of each ensemble, giving a pion mass of $m_\pi \sim 390$ MeV. The relevant quantities to assign to each ensemble that determine the impact of the finite lattice volume are $m_\pi L$ and $m_\pi T$, which for the four ensembles are $m_\pi L \sim 3.89, 4.86, 5.80$ and 7.73 respectively, and $m_\pi T \sim 8.89, 8.88, 8.84$ and 17.68 respectively.

Multiple light-quark propagators were calculated on each configuration in the four ensembles. The source locations were chosen randomly in an effort to minimize correlations among propagators. On the $\{16^3 \times 128,\ 20^3 \times 128,\ 24^3 \times 128,\ 32^3 \times 256\}$ ensembles, an average of {224, 364, 180, 174} propagators were calculated on each of {2001, 1195, 2215, 774} gauge-field configurations, to give a total number of $\sim \{4.5, 4.3, 3.9, 1.3\} \times 10^5$ light-quark propagators, respectively. The efffective mass plots (EMP's) for the nucleon on all of the time slices of each lattice ensemble are shown in fig. 1. They provide an indication of the precision of the present calculations.

## IV. THE VOLUME DEPENDENCE OF THE BARYON MASSES

The baryon masses that were extracted from the Lattice QCD calculations in the four different lattice volumes are given in table I. A detailed discussion of the fitting methods used in the analysis of the correlation functions is given in Refs. [7–9, 27].

### A. A Simplistic Analysis

It is useful to begin the analysis of the volume dependence of the baryon masses by performing a straightforward, but only partly motivated, fit to results of the Lattice QCD

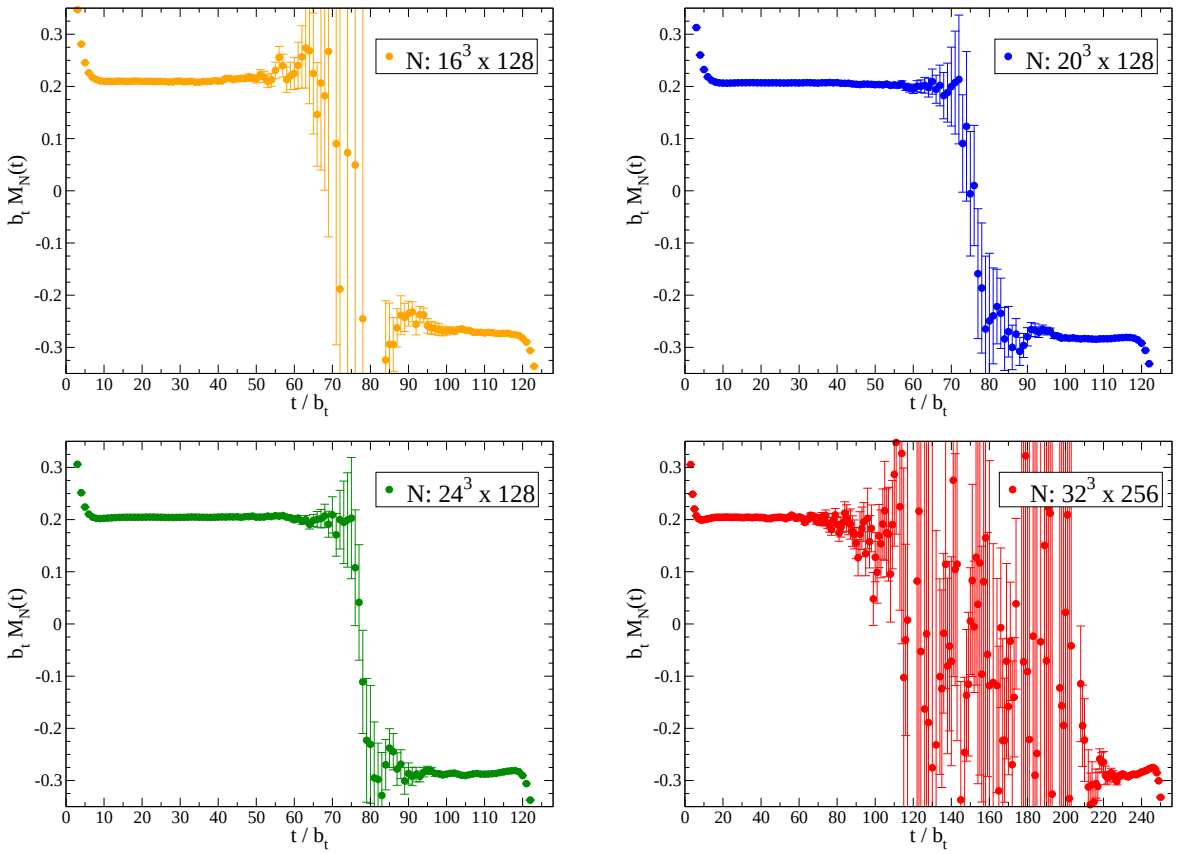


FIG. 1: The nucleon EMP's obtained in the four lattice volumes. Note that the temporal extent of the $32^3 \times 256$ ensemble is twice that of the other three ensembles.

TABLE I: Results from the Lattice QCD calculations in the four lattice volumes. (t.l.u. denotes temporal lattice units.)

| $L^3 \times T$ | $16^3 \times 128$ | $20^3 \times 128$ | $24^3 \times 128$ | $32^3 \times 256$ |
|---|---|---|---|---|
| $L$ (fm) | $\sim 2.0$ | $\sim$2.5 | $\sim$3.0 | $\sim$3.9 |
| $m_\pi L$ | 3.888(20)(01) | 4.8552(84)(35) | 5.799(16)(04) | 7.7347(74)(91) |
| $e^{-m_\pi L}$ | $\sim$0.0205 | $\sim$0.0078 | $\sim$0.0030 | $\sim$0.00044 |
| $\frac{1}{m_\pi L}\ e^{-m_\pi L}$ | $\sim 5.3 \times 10^{-3}$ | $\sim 1.6 \times 10^{-3}$ | $\sim 5.2 \times 10^{-4}$ | $\sim 5.7 \times 10^{-5}$ |
| $\frac{1}{(m_\pi L)^{3/2}}\ e^{-m_\pi L}$ | $\sim 2.7 \times 10^{-3}$ | $\sim 7.4 \times 10^{-4}$ | $\sim 2.2 \times 10^{-4}$ | $\sim 2.1 \times 10^{-5}$ |
| $m_\pi T$ | 8.89(16)(01) | 8.878(54)(22) | 8.836(85)(02) | 17.679(59)(73) |
| $e^{-m_\pi T}$ | $\sim 1.38 \times 10^{-4}$ | $\sim 1.39 \times 10^{-4}$ | $\sim 1.45 \times 10^{-4}$ | $\sim 2.10 \times 10^{-8}$ |
| $M_N$ (t.l.u.) | 0.21004(44)(85) | 0.20682(34)(45) | 0.20463(27)(36) | 0.20457(25)(38) |
| $M_\Lambda$ (t.l.u.) | 0.22446(45)(78) | 0.22246(27)(38) | 0.22074(20)(42) | 0.22054(23)(31) |
| $M_\Sigma$ (t.l.u.) | 0.22861(38)(67) | 0.22752(32)(43) | 0.22791(24)(31) | 0.22726(24)(43) |
| $M_\Xi$ (t.l.u.) | 0.24192(38)(63) | 0.24101(27)(38) | 0.23975(20)(32) | 0.23974(17)(31) |

calculations given in table I. As shown previously, the volume dependence of the mass of a given baryon can be calculated order-by-order in HB$\chi$PT. The formally-leading contribution

to the volume dependence of the mass of an octet baryon results from a one-loop diagram involving a pion and an octet baryon (ignoring for the moment the contribution from decuplet baryons). These one-loop contributions give rise to a volume dependence of the form given in eq. (4), $F_N^{(FV)}(m_\pi L)$. In obtaining this result, it is assumed that $m_\pi L$ is large, but significantly smaller than $m_X L$ where $m_X$ is the mass of other mesons, such as the kaon and the $\eta$, i.e. $m_K, m_\eta \gg m_\pi$. In the very-large volume limit, the finite-volume contributions are dominated by the first term in eq. (4). As such, it is useful, as a preliminary analysis, to fit a function of the form

$$M_B^{(V)}(m_\pi L) \;=\; M_B^{(\infty)} \;+\; c_B^{(V)} \; \frac{e^{-m_\pi L}}{m_\pi L} \tag{14}$$

to the results of the Lattice QCD calculations given in table I. One should view the parameter $c_B^{(V)}$ as providing an estimate of the strength of the axial coupling between the pion and the baryon. It should be stressed that the higher-order terms, beginning with terms of order $e^{-\sqrt{2}\ m_\pi L}/(m_\pi L)$, give a non-negligible contribution (relative to the uncertainties) in the $16^3 \times 128$ lattice volume, and a fit using the full function in eq. (4) leads to slightly reduced values of $c_B^{(V)}$ compared to those determined in the fits to eq. (14). The fits to each of the baryon masses are shown, along with the results of the Lattice QCD calculations, in fig. 2. The same vertical scale (but different intervals) has been used in the plots in fig. 2 in order for the reader to easily determine the relative size of the volume dependence of each of the masses. The values of the infinite-volume masses, $M_B^{(\infty)}$, and the coefficients of the leading volume dependences, $c_B^{(V)}$, are presented in table II. The nucleon is found to have the largest

TABLE II: The results of linear fits, of the form given in eq. (14), to the volume dependence of the baryon masses. $M_B^{(\infty)}$ is the infinite-volume extrapolation of the baryon mass and $c_B^{(V)}$ is the coefficient of $e^{-m_\pi L}/(m_\pi L)$. The first uncertainty is statistical, the second is the fitting systematic, and the third (where appropriate) is due to scale setting.

| Hadron | $M_B^{(\infty)}$ (t.l.u.) | $M_B^{(\infty)}$ (MeV) | $c_B^{(V)}$ (t.l.u.) | $c_B^{(V)}$ (MeV) |
|---|---|---|---|---|
| $M_N$ | 0.20427(17)(19) | 1149.8(1.0)(1.1)(7.5) | 1.15(09)(14) | $6.47(51)(78)(04) \times 10^3$ |
| $M_\Lambda$ | 0.22053(15)(21) | 1241.2(0.9)(1.1)(8.1) | 0.83(09)(12) | $4.64(53)(69)(03) \times 10^3$ |
| $M_\Sigma$ | 0.22744(17)(22) | 1280.3(1.0)(1.1)(8.3) | 0.21(09)(13) | $1.19(48)(71)(08) \times 10^3$ |
| $M_\Xi$ | 0.23972(13)(18) | 1349.4(0.8)(1.1)(8.8) | 0.47(08)(11) | $2.62(44)(60)(02) \times 10^3$ |

volume dependence. As the nucleon is comprised of light valence quarks only, it is expected to couple most strongly to pions, which should dominate its finite-volume modifications in the large-volume limit. It is expected that baryons with more strange quarks exhibit less volume sensitivity, and that the finite-volume mass shifts to the baryons, $\delta(FV)_B$, should naively satisfy the hierarchy

$$\delta(FV)_N \;>\; \delta(FV)_\Sigma \;,\; \delta(FV)_\Lambda \;>\; \delta(FV)_\Xi \quad . \tag{15}$$

The fit coefficients, $c_B^{(V)}$, given in table II are shown in fig. 3, where the expected hierarchy is approximately observed within the uncertainties of the calculation. The volume dependence of the $\Sigma$ is somewhat smaller than naive expectations would suggest.

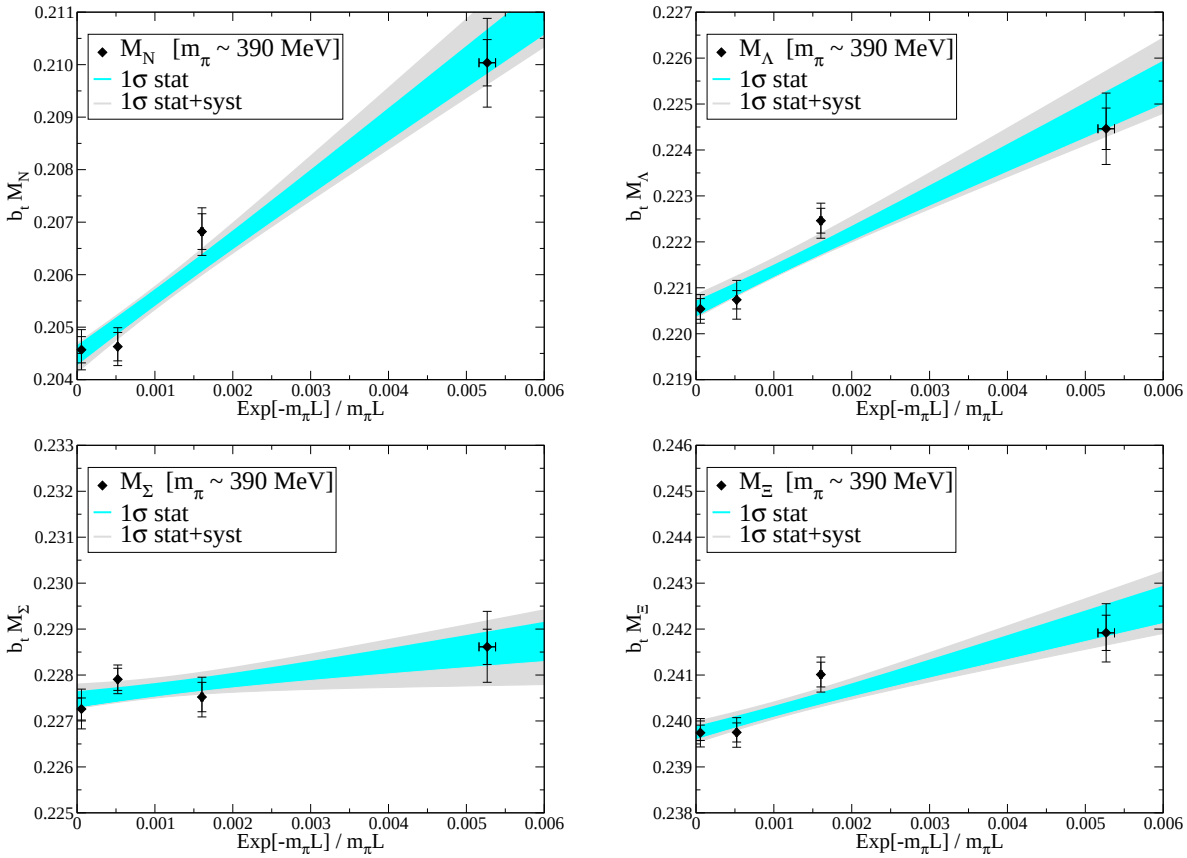


FIG. 2: The mass of the nucleon (upper left panel), the $\Lambda$ (upper right panel), the $\Sigma$ (lower left panel) and the $\Xi$ (lower right panel) as a function of $e^{-m_\pi L}/(m_\pi L)$. The points and associated uncertainties (blue) are the results of the Lattice QCD calculations. The dark (light) shaded region corresponds to the $1\sigma$ statistical uncertainty (statistical and systematic uncertainties combined in quadrature) associated with a fit of the form given in eq. (14).

### B. The Octet Baryons with NLO HB$\chi$PT

In this section we explore both $\mathrm{SU}(2)_L \otimes \mathrm{SU}(2)_R$ and $\mathrm{SU}(3)_L \otimes \mathrm{SU}(3)_R$ HB$\chi$PT predictions and fits to the results of the Lattice QCD calculations. The analyses are performed at NLO in the chiral expansion; unfortunately they do not provide significant constraints on the counterterms that appear beyond NLO in HB$\chi$PT. Our strategy in these analyses is to use the octet-octet axial couplings and the octet-decuplet mass splittings from experimental data and Lattice QCD results, and fit the octet-decuplet axial couplings and the baryon masses in the infinite-volume limit to the results of the Lattice QCD calculations, given in table I, using two-flavor HB$\chi$PT. Inserting these fit values into the full three-flavor finite-volume corrections gives a measure of the relevance of kaon and $\eta$ loops. The goal is to determine the extent to which two- and three-flavor HB$\chi$PT describe the volume dependence of the results of the Lattice QCD calculations. And, of course, it is of interest to determine whether any significant constraints can be placed on the –with few exceptions, rather poorly known– axial coupling constants of the baryons by studying finite-volume effects.

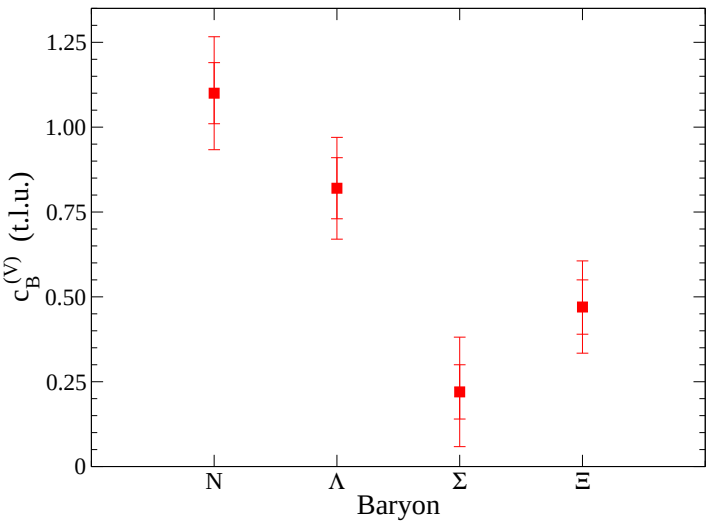


FIG. 3: The fit values of $c_B^{(V)}$, the coefficient of $e^{-m_\pi L}/(m_\pi L)$ in eq. (14), given in table II for each of the octet baryons.

### 1. *Parameter Set*

Lattice QCD calculations show that the nucleon axial coupling, $g_A$, is essentially independent of the light-quark masses [28–31], and so in the following we use the experimentally-determined value $g_A = 1.26$ as well as the central values of $g_{\Lambda\Sigma}$, $g_{\Sigma\Sigma}$, and $g_{\Xi\Xi}$ determined from Lattice QCD calculations [32] interpolated to the appropriate pion mass, or from the tree-level SU(3) relations between axial couplings at the physical pion mass (which are consistent with each other)

$$g_{\Lambda\Sigma} = 1.58(20) \quad , \quad g_{\Sigma\Sigma} = 0.900(30) \quad , \quad g_{\Xi\Xi} = 0.262(13) \quad . \tag{16}$$

While the pion decay constant, $f_\pi$, is experimentally determined to be $f_\pi \sim 132$ MeV at the physical light-quark masses, Lattice QCD calculations have determined how it depends upon the light-quark masses, and at $m_\pi \sim 390$ MeV its value is $f_\pi \sim 150$ MeV [33–36]. We take the baryon mass splittings determined from octet and decuplet correlation functions calculated on the $32^3 \times 256$ ensemble[4]:

$$\begin{aligned}
&\Delta_{\Delta N} = 298 \text{ MeV} \quad , \quad \Delta_{\Sigma N} = 128 \text{ MeV} \quad , \quad \Delta_{\Lambda N} = 90 \text{ MeV} \quad , \quad \Delta_{\Sigma^* N} = 427 \text{ MeV} \ ; \\
&\Delta_{\Sigma\Lambda} = 38 \text{ MeV} \quad , \quad \Delta_{\Sigma^*\Lambda} = 336 \text{ MeV} \quad , \quad \Delta_{\Xi\Lambda} = 108 \text{ MeV} \quad , \quad \Delta_{\Xi^*\Lambda} = 406 \text{ MeV} \ ; \\
&\Delta_{\Xi\Sigma} = 69 \text{ MeV} \quad , \quad \Delta_{\Sigma^*\Sigma} = 298 \text{ MeV} \quad , \quad \Delta_{\Delta\Sigma} = 229 \text{ MeV} \quad , \quad \Delta_{\Xi^*\Sigma} = 368 \text{ MeV} \ ; \\
&\Delta_{\Xi^*\Xi} = 298 \text{ MeV} \quad , \quad \Delta_{\Sigma^*\Xi} = 228 \text{ MeV} \quad , \quad \Delta_{\Omega\Xi} = 367 \text{ MeV} \ .
\end{aligned} \tag{17}$$

For the $\mathrm{SU}(3)_L \otimes \mathrm{SU}(3)_R$ HB$\chi$PT analysis, the SU(3)-symmetric axial couplings are fixed to the central values of the best-fit experimental values: $D = 0.79$, $F = 0.47$ and

[4] We do not quote uncertainties on these determinations as they do not significantly affect the NLO HB$\chi$PT fits.

$\mathcal{C} = 1.47$ [37]. Further, the decay constants and masses are set to $f_K = f_\eta = 160$ MeV and the lattice-determined values $m_K = 544$ MeV, and $m_\eta = 587$ MeV (the latter determined from $m_\pi$ and $m_K$ via the Gell-Mann–Okubo (GMO) relation), respectively.

### 2. *The Nucleon Mass*

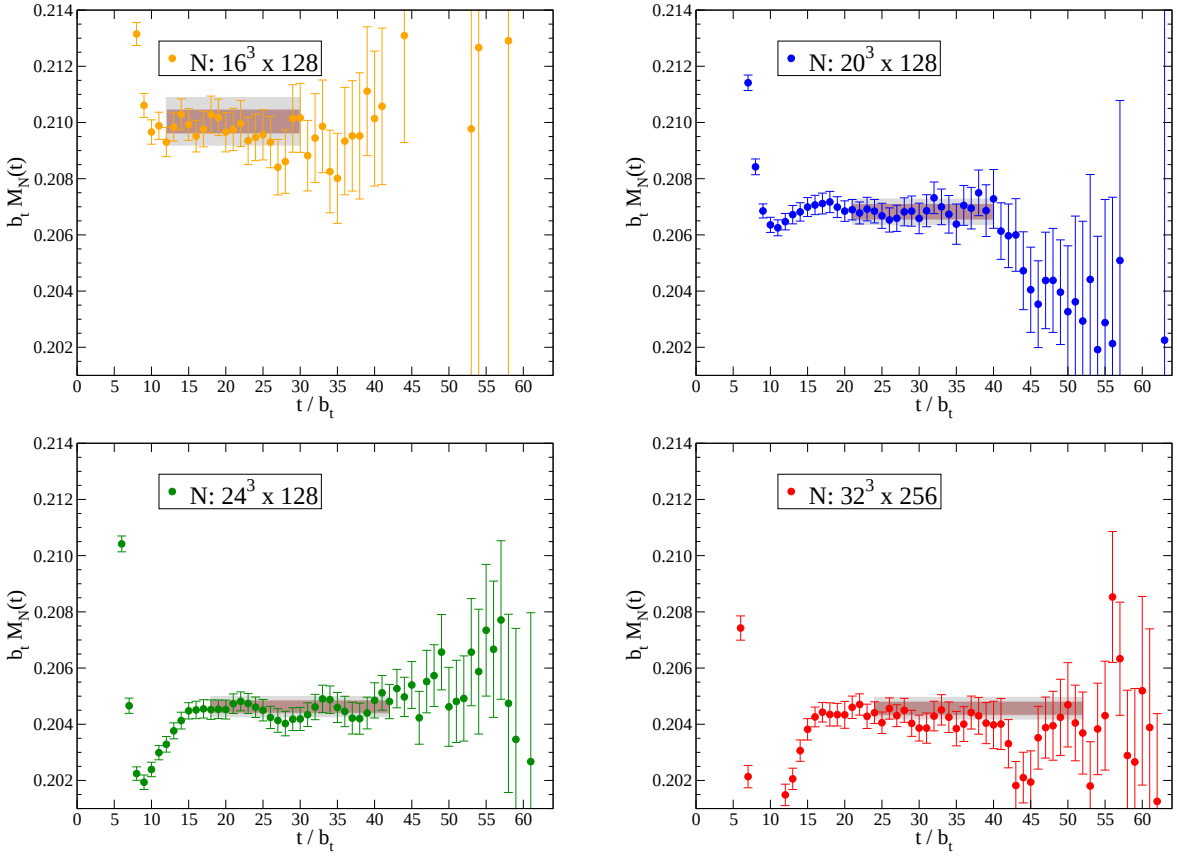


FIG. 4: The Nucleon EMP's determined on the four lattice ensembles used in this work. They each result from linear combinations of different correlation functions that optimize the plateau of the ground state. Note that the y-axis scale is the same in all four panels.

The nucleon EMP's and fits to the mass plateaus obtained from the results of the Lattice QCD calculations on the four lattice ensembles are shown in fig. 4. With the input parameters given in subsection IV B 1, a two-parameter fit to the nucleon mass data, given in table I, can be performed in two-flavor HB$\chi$PT to determine the infinite-volume value of the nucleon mass, $M_N^{(\infty)}$, and the value of the $\Delta N\pi$ axial coupling, $g_{\Delta N\pi}$. While there have been many previous determinations of $g_{\Delta N\pi}$, we treat it as a fit parameter and compare its value with the previous extractions. Fitting the expression in eq. (3) to the results given in table I gives the fit-regions shown in fig. 5, and fit values of

$$M_N^{(\infty)} = 0.20455(19)(17) \text{ t.l.u} \quad , \quad |g_{\Delta N\pi}| = 2.80(18)(21) \quad . \tag{18}$$

The ratio of couplings

$$\frac{|g_{\Delta N\pi}|}{g_A} \;=\; 2.22(14)(17) \quad , \tag{19}$$

can be compared with the value of $|g_{\Delta N\pi}|/g_A = 1.56(06)$ [38] [5] extracted from an analysis of experimentally-measured $\pi N$ scattering phase shifts. The difference between these two values is significant, but as the two extractions have been performed at two different unphysical pion masses, little can be concluded. On the other hand, direct Lattice QCD calculations of $|g_{\Delta N\pi}|/g_A$ have been performed [39, 40] over a range of pion masses [6]. One such calculation performed with a pion mass in the vicinity of $m_\pi \sim 390$ MeV gives $|g_{\Delta N\pi}|/g_A = 1.47(19)$. The finite-volume corrections to the nucleon mass resulting from this value of the coupling is shown as the dashed (red) curve in fig. 5, and clearly the contribution from the $N\pi$ and the $\Delta\pi$ intermediate states constitute a large fraction of the finite-volume shift of the nucleon mass. Given the size of the pion mass in the present calculations, $m_\pi/M_N \sim 0.35$, we anticipate that higher orders in HB$\chi$PT will change the finite-volume corrections at the $\sim 30\%$ level, consistent with the difference between the results of the lattice QCD calculations and NLO in HB$\chi$PT [7]. A next-to-next-to-leading order (NNLO) calculation of the finite-volume contributions to the nucleon mass in HB$\chi$PT, accompanied by more precise Lattice QCD calculations over a range of lattice volumes and quark masses, is required in order to improve upon this determination of $g_{\Delta N\pi}$ [8].

With these fit parameters and the parameter set previously defined in subsection IV B 1, the effect of kaon and $\eta$ loops can be estimated by including the finite-volume corrections given in eq. (9), the results of which are shown in fig. 5. The contributions from the strange-baryon and strange-meson intermediate states are estimated to be small, and somewhat improve the agreement between theory and the Lattice QCD calculation. Including them in the fit of $g_{\Delta N\pi}$ to the results of the Lattice QCD calculation gives $|g_{\Delta N\pi}|/g_A = 2.10(15)(20)$, which is to be compared with the result in eq. (19).

As NLO HB$\chi$PT reproduces most of the volume dependence of the nucleon mass at $m_\pi \sim 390$ MeV, and is expected to become more accurate at lighter pion masses, it is useful to use the NLO expression to estimate the size of the finite-volume contributions to the nucleon mass at the pion masses other than the current one. In fig. 6 we show the finite-volume contributions to the nucleon mass that are predicted at NLO in HB$\chi$PT for $m_\pi \sim 390, 230$ and 140 MeV. This makes clear that finite-volume effects are expected to

---

[5] The value of $|g_{\Delta N\pi}|/g_A$ in Ref. [38] has been divided by $\sqrt{2}$ in order to match the definition of $g_{\Delta N\pi}$ employed in defining eq. (3) [17].

[6] The two methods employed in Ref. [40] suggest that there may be a relatively large systematic uncertainty in their value of $|g_{\Delta N\pi}|/g_A$ beyond that quoted.

[7] If instead of using $f_\pi \sim 150$ MeV to evaluate the NLO HB$\chi$PT result, the value at the physical pion mass, $f_\pi \sim 132$ MeV is used, then a value of $|g_{\Delta N\pi}|/g_A = 1.76(18)$ is obtained, consistent within uncertainties with the extraction from the matrix element of the axial current [39]. The ambiguity in the value of the decay constant that is used in the NLO contribution will be parametrically reduced by a NNLO calculation.

[8] An alternative, efficient way of capturing the bulk of the volume dependence is to insert the forward $\pi$N scattering amplitude, calculated in HB$\chi$PT with explicit $\Delta$ degrees of freedom into eq. (1) [41]. This procedure has been shown to work well for the $\pi$ mass volume dependence [42].

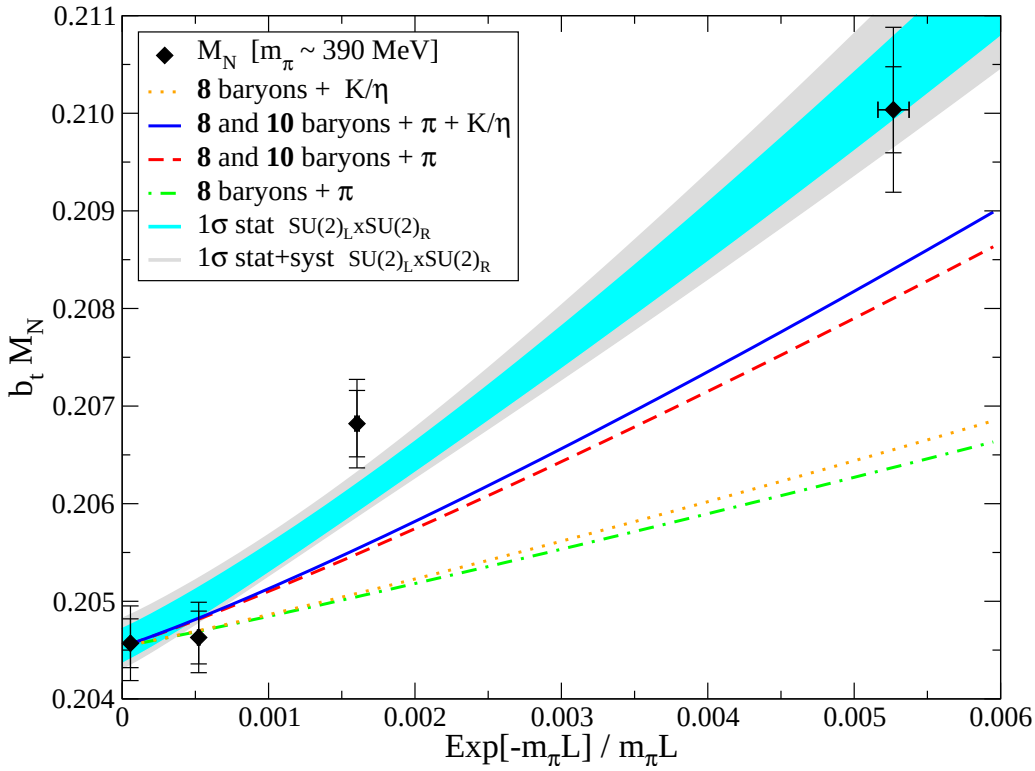


FIG. 5: The mass of the nucleon as a function of $e^{-m_\pi L}/(m_\pi L)$. The dark (light) grey shaded region corresponds to the $1\sigma$ statistical uncertainty (statistical and systematic uncertainties combined in quadrature) resulting from fitting $M_N^{(\infty)}$ and $g_{\Delta N\pi}$. Using this value of $M_N^{(\infty)}$, the dot-dashed curve (green) corresponds to the contribution from octet baryons and pions, the dotted curve (orange) corresponds to the contribution from octet baryons and kaons or an $\eta$, the dashed curve (red) corresponds to the contribution from octet and decuplet baryons and pions, and the solid curve (blue) corresponds to the contribution from octet and decuplet baryons and pions, kaons or an $\eta$.

be significantly smaller at the lighter pion masses for fixed $m_\pi L$. For instance, the value of $m_\pi L$, estimated at NLO in HB$\chi$PT, for which the finite-volume contribution to the nucleon mass is $\delta M_N^{(FV)} = 10$ MeV at $m_\pi = 390$ MeV is $m_\pi L \sim 4.4$. Similarly, the values of $m_\pi L$ for which the finite-volume contributions to the nucleon mass are $\delta M_N^{(FV)} = 1$ MeV at $m_\pi = 390, 230$ and 140 MeV are $m_\pi L \sim 6.2, 4.7$ and 3.9, respectively. For $\delta M_N^{(FV)} = 100$ keV, the corresponding values are $m_\pi L \sim 8.0$, 6.4, and 5.8, respectively. Given that the deuteron binding energy and nuclear excitation energies are in the MeV regime, the estimates indicate that $m_\pi L \gtrsim 2\pi$ is required at the physical pion mass in order to eliminate contamination from this class of exponentially-suppressed finite-volume effects that contaminate the extraction of phase shifts and binding energies from Lattice QCD calculations.

### *3. The Λ Mass*

The Λ EMP's and fits to the mass plateaus obtained from the results of the Lattice QCD calculations for the four lattice ensembles are shown in fig. 7. The fit values of the Λ masses

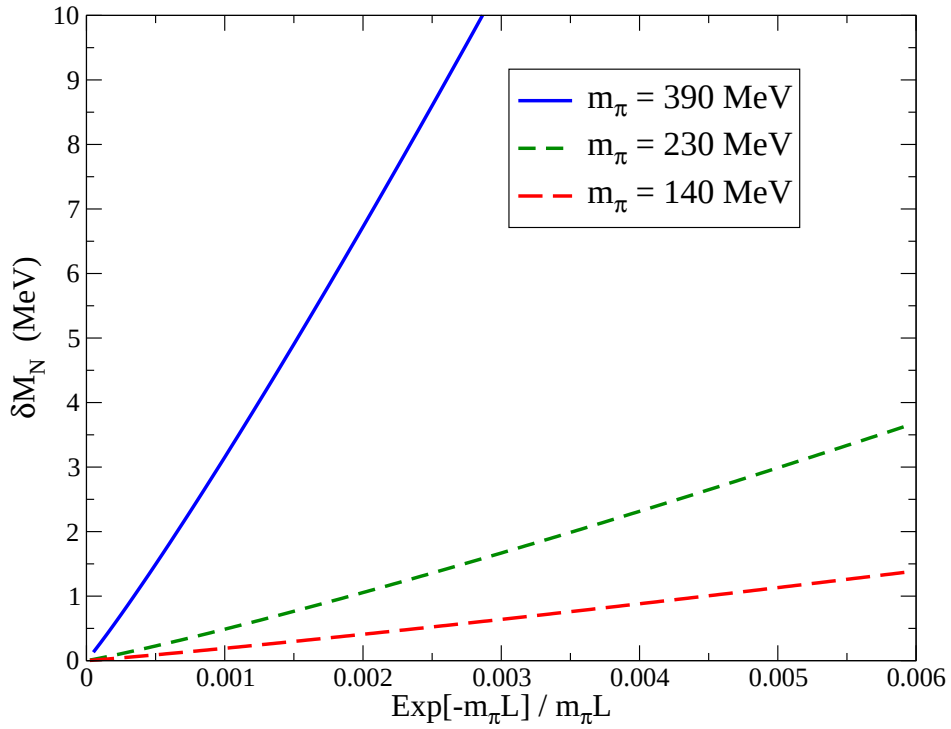


FIG. 6: Estimates of the finite-volume contributions to the nucleon mass at NLO in HB$\chi$PT for $m_\pi = 390$ MeV (upper, blue, solid, which corresponds to the red dashed curve in fig. 5), $m_\pi = 230$ MeV (middle, green, dotted), and $m_\pi = 140$ MeV (lower, red, dashed).

in the four lattice volumes are given in table I, and are shown as the points with uncertainties in fig. 8. The shaded regions in fig. 8 show the results of the $\mathrm{SU}(2)_L \otimes \mathrm{SU}(2)_R$ HB$\chi$PT fit to the volume dependence of the $\Lambda$ mass using eq. (6) and the value of $g_{\Sigma\Lambda}$ given in eq. (16). The fit gives

$$M_\Lambda^{(\infty)} \;=\; 0.22064(15)(19)\ \text{t.l.u} \quad , \quad |g_{\Sigma^*\Lambda\pi}| \;=\; 2.21(16)(23) \quad . \tag{20}$$

If instead of fitting $g_{\Sigma^*\Lambda\pi}$, flavor SU(3) symmetry is used to relate it to $g_{\Delta N\pi}$, $g_{\Sigma^*\Lambda\pi} = g_{\Delta N\pi}/\sqrt{2} = 1.3$, then the contribution from $\Sigma$ intermediate states and from $\Sigma$ and $\Sigma^*$ intermediate states are shown as the dot-dashed (green) and dashed (red) curves in fig. 8, respectively. Comparing these expectations with the results of the Lattice QCD calculations, manifested in the fit value of $g_{\Sigma^*\Lambda\pi}$ being $\sim 40\%$ larger than phenomenological expectations, indicates that higher orders in two-flavor $\chi$PT are important, or that the strange quark plays a role in the finite-volume contributions through kaons or an $\eta$.

As with the nucleon, we can now estimate the effects of kaon and $\eta$ loops by including the finite-volume corrections given in eq. (10). This gives rise to the curves shown in fig. 8. (Note that the same values for the input parameters are used to generate the curves in fig. 8 as are used in the case of the nucleon). The dot-dashed (green) and dashed (red) curves are the contributions from pions, while the dotted (orange) and solid (blue) curves correspond to the sum of contributions from pions, kaons and an $\eta$. The pions make the largest contribution to the volume dependence of the mass of the $\Lambda$, but, unlike in the case of the nucleon, the kaons and $\eta$ contribute significantly. It is interesting to note that the NLO contribution in three-flavor HB$\chi$PT (blue curve) agrees well with the results of the

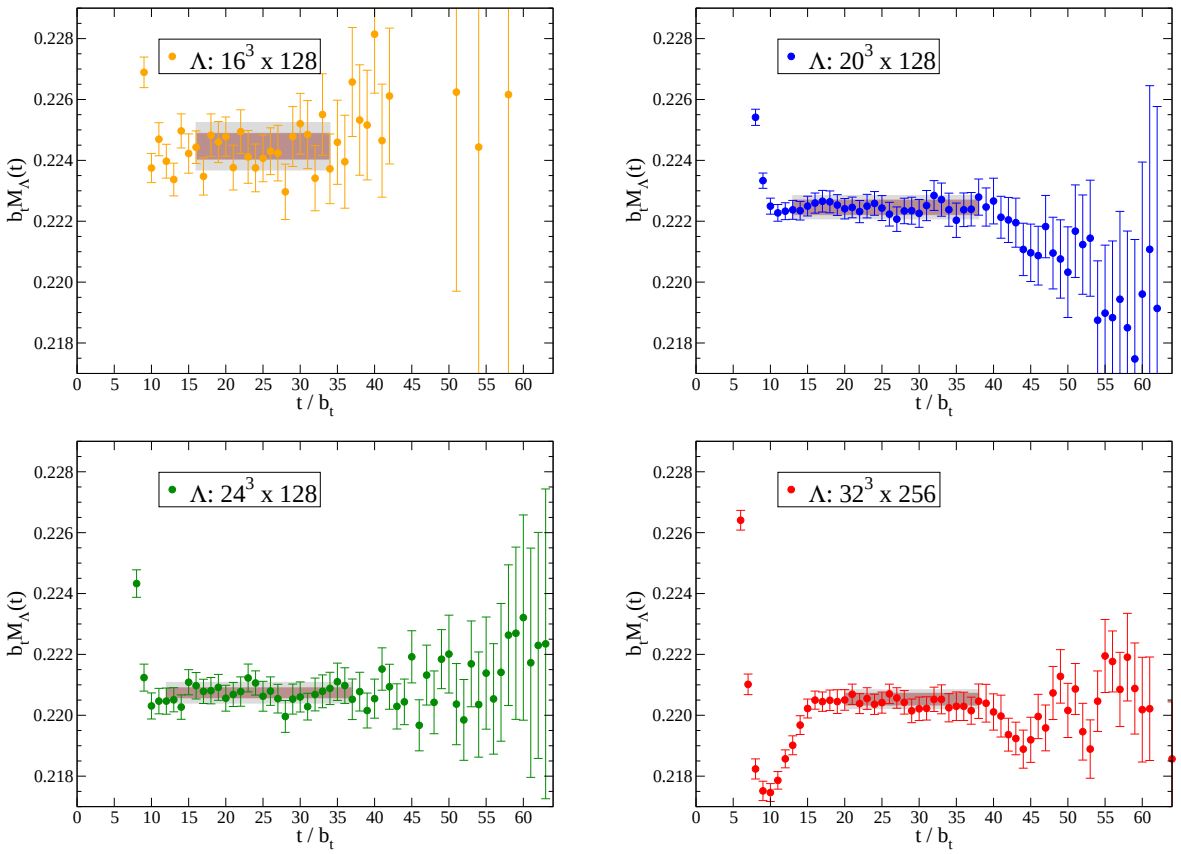


FIG. 7: The Λ EMP's determined on the four lattice ensembles used in this work. They each result from linear combinations of different correlation functions that optimize the plateau of the ground state. Note that the y-axis scale is the same in all four panels.

Lattice QCD calculation. However, NLO HB$\chi$PT is expected to be modified at the $\sim 30\%$ level by higher orders in the expansion.

### *4. The Σ Mass*

The Σ EMP's and fits to the mass plateaus obtained from the results of the Lattice QCD calculations on the four lattice ensembles are shown in fig. 9. The fit values of the Σ masses in the four lattice volumes are given in table I, and are shown as the points with uncertainties in fig. 10. The shaded regions in fig. 10 show the results of the $\mathrm{SU}(2)_L \otimes \mathrm{SU}(2)_R$ HB$\chi$PT fit to the volume dependence of the Σ mass using eq. (7) with the axial couplings given in eq. (16). The fit gives

$$M_\Sigma^{(\infty)} \;=\; 0.22747(17)(19)\ \text{t.l.u} \quad , \quad |g_{\Sigma^*\Sigma\pi}| \;<\; 1.38[1.90] \quad , \tag{21}$$

where we have quoted a 68% confidence interval for $g_{\Sigma^*\Sigma\pi}$ including statistical errors and statistical and systematic errors added in quadrature (bracketed). If instead of fitting $g_{\Sigma^*\Sigma\pi}$, the SU(3) relation is used, $g_{\Sigma^*\Sigma\pi} = g_{\Delta N\pi}/\sqrt{3} = 1.07$, then the contribution from Σ, Λ intermediate states and from Σ, Λ and $\Sigma^*$ intermediate states are shown as the dot-dashed (green) and dashed (red) curves in fig. 10, respectively. The NLO $\mathrm{SU}(3)_L \otimes \mathrm{SU}(3)_R$ HB$\chi$PT

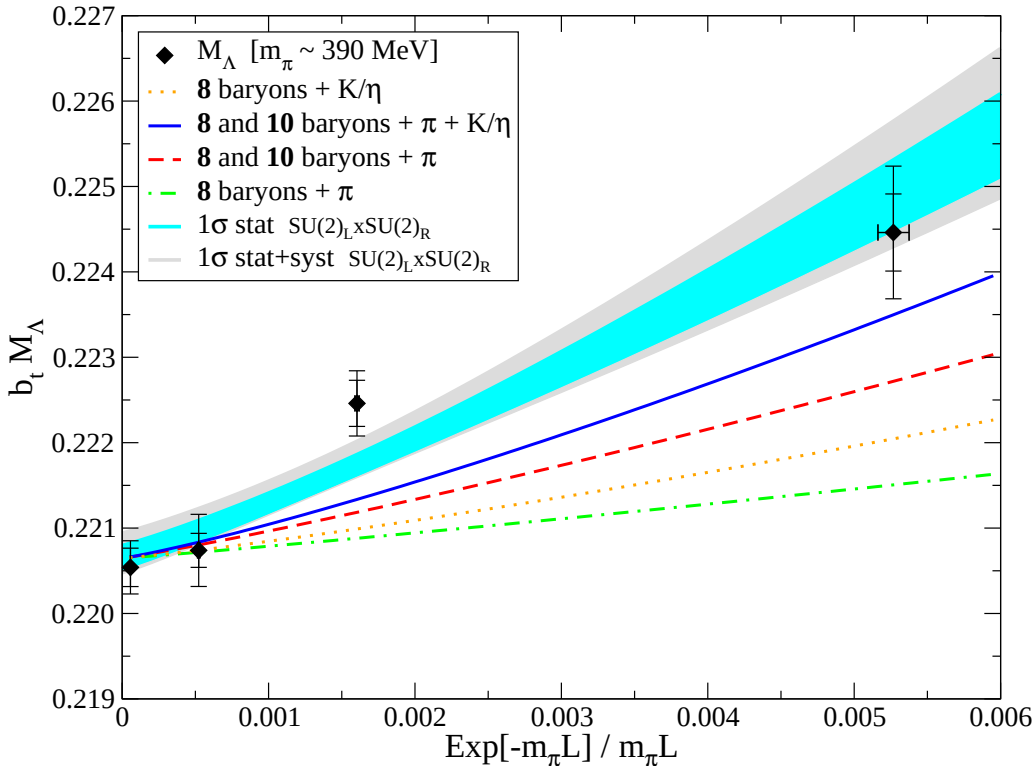


FIG. 8: The mass of the $\Lambda$ as a function of $e^{-m_\pi L}/(m_\pi L)$. The dark (light) grey shaded region corresponds to the $1\sigma$ statistical uncertainty (statistical and systematic uncertainties combined in quadrature) resulting from fitting $M_\Lambda^{(\infty)}$ and $g_{\Sigma^*\Lambda\pi}$. Using this value of $M_\Lambda^{(\infty)}$, the dot-dashed curve (green) corresponds to the contribution from octet baryons and pions, the dotted curve (orange) corresponds to the contribution from octet baryons and kaons or an $\eta$, the dashed curve (red) corresponds to the contribution from octet and decuplet baryons and pions, and the solid curve (blue) corresponds to the contribution from octet and decuplet baryons and pions, kaons or an $\eta$.

prediction (blue curve) is somewhat higher than the result of the Lattice QCD calculation in the smallest volume, but not significantly so. It should be added that the SU(3) value of the coupling constant, $g_{\Sigma^*\Sigma\pi} = 1.07$ is consistent with the confidence interval extracted from the $\mathrm{SU}(2)_L \otimes \mathrm{SU}(2)_R$ fit, given in eq. (21).

The volume dependence of the $\Sigma$ mass is found to be somewhat smaller than that of the $\Lambda$ mass. This is consistent with the prediction of NLO $\mathrm{SU}(3)_L \otimes \mathrm{SU}(3)_R$ HB$\chi$PT, which is largely driven by the coupling to the decuplet intermediate states. The difference in the couplings to the decuplet, given in eq. (13), is sufficient to explain the difference in volume dependence.

### 5. *The $\Xi$ Mass*

The $\Xi$ EMP's and fits to the results of the Lattice QCD calculations on the four lattice ensembles are shown in fig. 11. The fit values of the $\Xi$ masses in the four lattice volumes are given in table I, and are shown as the points with uncertainties in fig. 12. The shaded regions in fig. 12 show the results of the $\mathrm{SU}(2)_L \otimes \mathrm{SU}(2)_R$ HB$\chi$PT fit to the volume dependence of

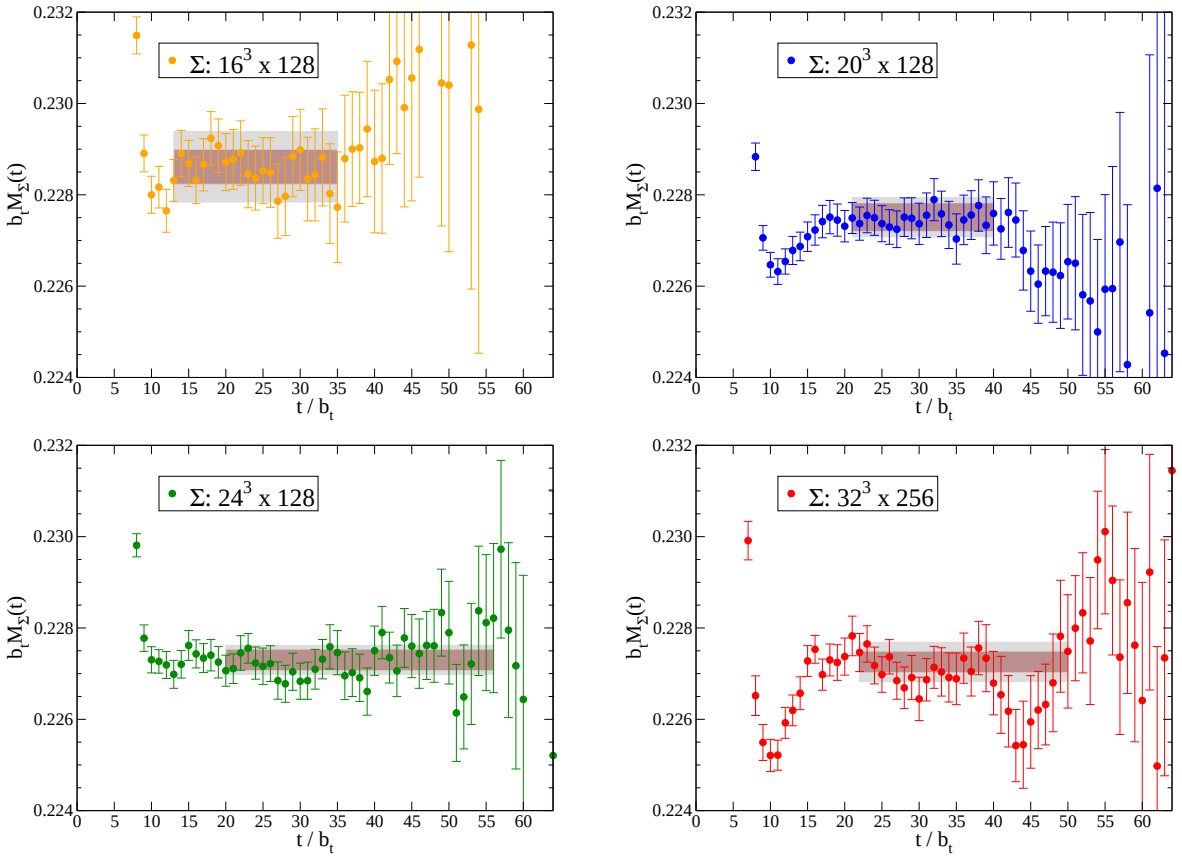


FIG. 9: The $\Sigma$ EMP's determined on the four lattice ensembles used in this work. They each result from linear combinations of different correlation functions that optimize the plateau of the ground state. Note that the y-axis scale is the same in all four panels.

the $\Xi$ mass using eq. (8). The fit parameters are

$$M_\Xi^{(\infty)} \;=\; 0.23978(12)(18)\ \text{t.l.u} \quad , \quad |g_{\Xi^*\Xi\pi}| \;=\; 2.49(23)(35) \quad . \tag{22}$$

If instead of fitting $g_{\Xi^*\Xi\pi}$, the estimates from other observables are used, $g_{\Xi^*\Xi\pi} = g_{\Delta N\pi}/2 = 0.93$ [43], the contribution from $\Xi$ intermediate states and from $\Xi$ and $\Xi^*$ intermediate states are shown as the dot-dashed (green) and dashed (red) curves in fig. 12, respectively. Comparing the expectations with the results of the Lattice QCD calculations, manifested in the fit value of $g_{\Xi^*\Xi\pi}$ being more than twice expectations, suggest that the pionic contributions do not dominate the finite-volume corrections, even after considering contributions from higher orders in $\text{SU}(2)_L \otimes \text{SU}(2)_R$ HB$\chi$PT. As the $\Xi$ carries two strange quarks, one expects kaon and $\eta$ loops to make relatively larger finite-volume contributions to the $\Xi$ mass than to the nucleon, $\Lambda$ and $\Sigma$ masses.

The NLO $\text{SU}(3)_L \otimes \text{SU}(3)_R$ HB$\chi$PT prediction from eq. (12) gives rise to the curves shown in fig. 12. The dot-dashed (green) and dashed (red) curves are the contributions from pions, while the dotted (orange) and solid (blue) curves correspond to the sum of contributions from pions, kaons and an $\eta$. HB$\chi$PT predicts that it is the kaons and $\eta$ that dominate the finite-volume contributions to the $\Xi$ mass. The exponential suppression of the kaon and $\eta$ contributions is not sufficient to overcome the relatively large axial coupling constants

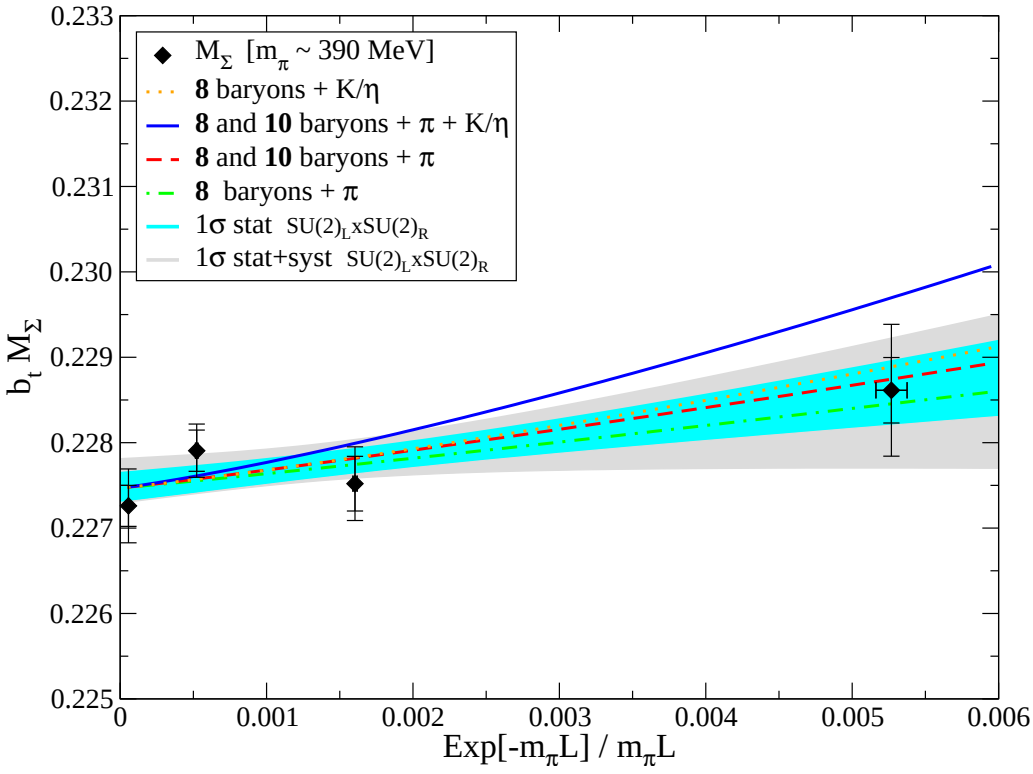


FIG. 10: The mass of the $\Sigma$ as a function of $e^{-m_\pi L}/(m_\pi L)$. The dark (light) grey shaded region corresponds to the $1\sigma$ statistical uncertainty (statistical and systematic uncertainties combined in quadrature) resulting from fitting $M_\Sigma^{(\infty)}$ and $g_{\Sigma^*\Sigma\pi}$. Using this value of $M_\Sigma^{(\infty)}$, the dot-dashed curve (green) corresponds to the contribution from octet baryons and pions, the dotted curve (orange) corresponds to the contribution from octet baryons and kaons or an $\eta$, the dashed curve (red) corresponds to the contribution from octet and decuplet baryons and pions, and the solid curve (blue) corresponds to the contribution from octet and decuplet baryons and pions, kaons or an $\eta$.

at this pion mass. These results suggest that NLO $\mathrm{SU}(3)_L \otimes \mathrm{SU}(3)_R$ HB$\chi$PT provides a good description of the finite-volume modifications to the $\Xi$ mass. Again, one expects NLO HB$\chi$PT to provide an estimate of the finite volume effects that would be modified at the $\sim 30\%$ level by higher orders in the expansion.

### *6. Summary*

The infinite-volume values of the octet-baryon masses fit from the Lattice QCD data using HB$\chi$PT are consistent (almost identical) with the infinite-volume values extracted from the simple phenomenological fits presented above (see table III for a summary). However, there are several important lessons that one learns from the HB$\chi$PT analysis of the volume dependence of the octet-baryon masses. First, by comparing, for instance, the dashed (red) and dot-dashed (green) curves in fig. 5, fig. 8, fig. 10 and fig. 12, one sees the relevance of the octet-decuplet axial transitions in the description of the finite-volume effects. We conclude that HB$\chi$PT with the decuplet states integrated out does not provide a reliable description of the finite-volume effects at NLO at this pion mass. Second, by comparing, for instance,

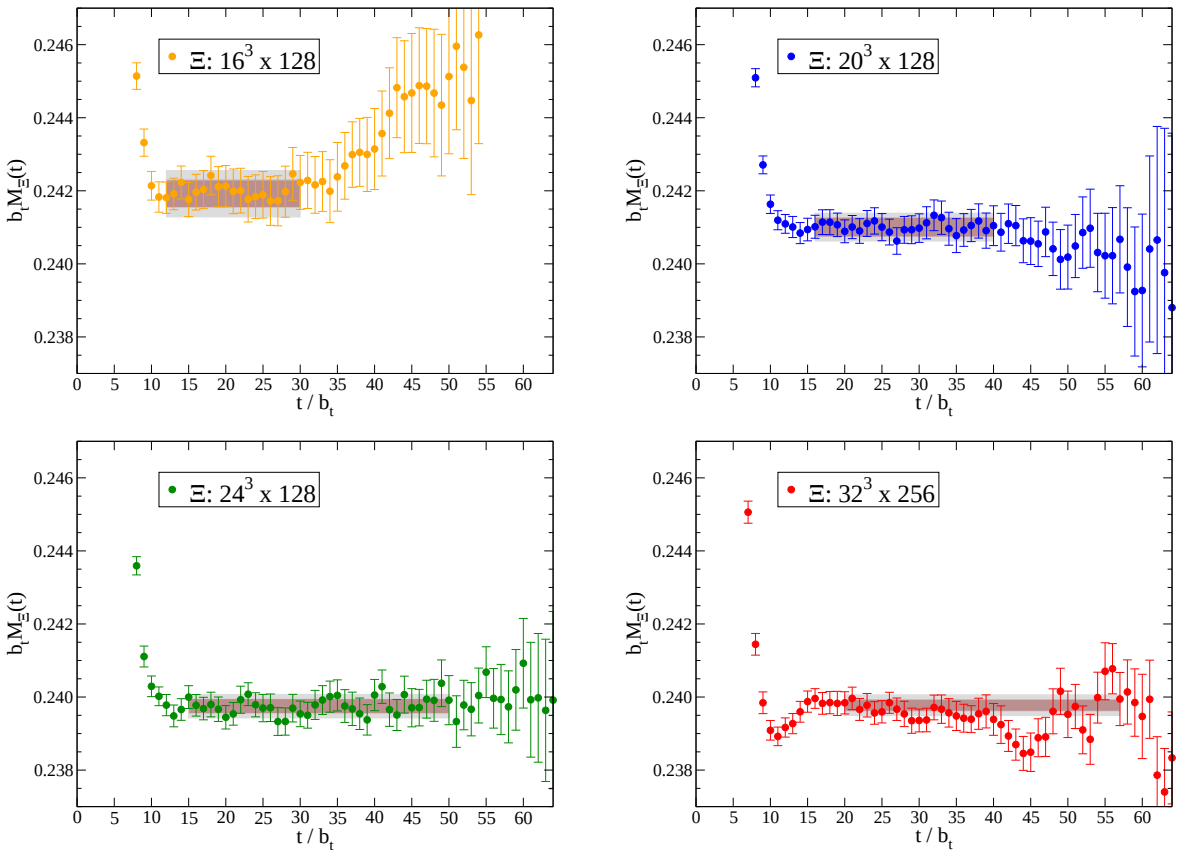


FIG. 11: The Ξ EMP's determined on the four lattice ensembles used in this work. They each result from linear combinations of different correlation functions that optimize the plateau of the ground state. Note that the y-axis scale is the same in all four panels.

the solid (blue) curve and the dashed (red) curve in fig. 5, fig. 8, fig. 10 and fig. 12, one sees the relative importance of fluctuations to intermediate states involving kaons and/or $\eta$, which are not captured in the two-flavor chiral expansion. While these effects are small in the case of the nucleon, they are significant for the hyperons at the heavy pion mass at which the Lattice calculations were performed. Therefore, while $\mathrm{SU}(2)_L \otimes \mathrm{SU}(2)_R$ HB$\chi$PT is adequate for the nucleon, $\mathrm{SU}(3)_L \otimes \mathrm{SU}(3)_R$ HB$\chi$PT is necessary to account for the finite-volume effects experienced by the hyperons [9]. And thus, the fit hyperon axial couplings presented in table III should not be considered reliable. This is, of course, due to $m_K - m_\pi$ not being large enough, and the $\mathrm{SU}(2)_L \otimes \mathrm{SU}(2)_R$ fits for the hyperons are expected to improve as the physical pion mass is approached. It is important to emphasize that we have not propagated the uncertainties associated with the input axial couplings and baryon mass splittings, as we have found that the resulting uncertainties in the fit quantities are smaller than the expected size of NNLO effects. The various curves in fig. 5, fig. 8, fig. 10 and fig. 12 become bands when the input parameter uncertainties are included.

[9] We caution that reproducing the calculated volume dependence using HB$\chi$PT does not imply that the quark-mass dependence itself is under control. Indeed it is well known that $\mathrm{SU}(3)_L \otimes \mathrm{SU}(3)_R$ HB$\chi$PT converges poorly for certain quantities [44–46].

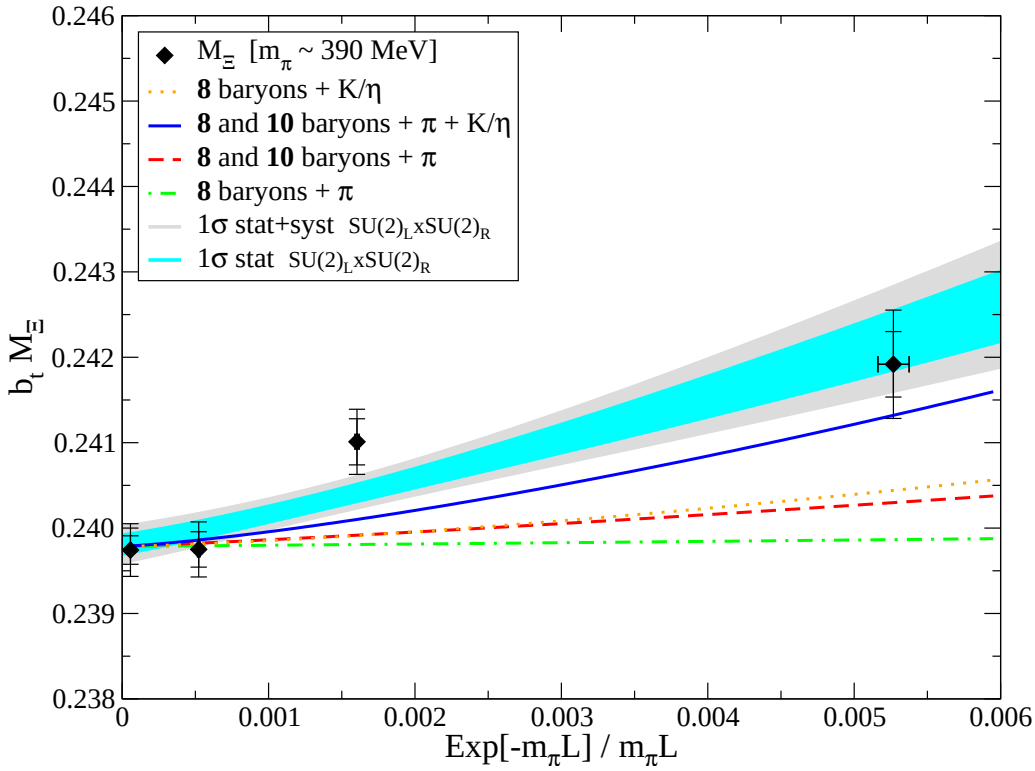


FIG. 12: The mass of the $\Xi$ as a function of $e^{-m_\pi L}/(m_\pi L)$. The dark (light) grey shaded region corresponds to the $1\sigma$ statistical uncertainty (statistical and systematic uncertainties combined in quadrature) resulting from fitting $M_\Xi^{(\infty)}$ and $g_{\Xi^*\Xi\pi}$. Using this value of $M_\Xi^{(\infty)}$, the dot-dashed curve (green) corresponds to the contribution from octet baryons and pions, the dotted curve (orange) corresponds to the contribution from octet baryons and kaons or an $\eta$, the dashed curve (red) corresponds to the contribution from octet and decuplet baryons and pions, and the solid curve (blue) corresponds to the contribution from octet and decuplet baryons and pions, kaons or an $\eta$.

TABLE III: The results of NLO $\mathrm{SU}(2)_L \otimes \mathrm{SU}(2)_R$ HB$\chi$PT fits to the volume dependence of the baryon masses. $M_B^{(\infty)}$ is the infinite-volume extrapolation of the baryon mass. The first uncertainty is statistical, the second is the fitting systematic, and the third (where appropriate) is due to scale setting. The uncertainties in the input axial couplings and baryon mass splittings have not been propagated, as discussed in the text.

| Hadron | $M_B^{(\infty)}$ (t.l.u.) | $M_B^{(\infty)}$ (MeV) | Axial Coupling |
|---|---|---|---|
| $M_N$ | 0.20455(19)(17) | 1151.3(1.1)(1.0)(7.5) | $\lvert g_{\Delta N\pi}\rvert$ = 2.80(18)(21) |
| $M_\Lambda$ | 0.22064(15)(19) | 1241.9(0.8)(1.1)(8.1) | $\lvert g_{\Sigma^*\Lambda\pi}\rvert$ = 2.21(16)(23) |
| $M_\Sigma$ | 0.22747(17)(19) | 1280.3(1.0)(1.1)(8.3) | $\lvert g_{\Sigma^*\Sigma\pi}\rvert$ < 1.38[1.90] |
| $M_\Xi$ | 0.23978(12)(18) | 1349.6(0.7)(1.0)(8.8) | $\lvert g_{\Xi^*\Xi\pi}\rvert$ = 2.49(23)(35) |

### C. Combinations of Masses

In addition to examining the volume dependence of the baryon masses, it is interesting to explore the volume dependence of certain combinations of the masses. In order to minimize both statistical and systematic uncertainties in determining various combinations of masses from the Lattice QCD calculation, in each case a correlation function is formed from products or ratios of the individual baryon correlation functions under a jackknife or bootstrap procedure, from which the combination of masses is extracted.

#### *1. The Centroid of the Octet*

The centroid of the baryon octet is the sum of the masses weighted by the isospin degeneracy of each state,

$$M_{\mathbf{8}} \;=\; \frac{1}{8}M_\Lambda + \frac{3}{8}M_\Sigma + \frac{1}{4}M_N + \frac{1}{4}M_\Xi \quad . \tag{23}$$

The results of the Lattice QCD calculations are shown in fig. 13, along with the results of a simple fit of the form described in subsection IV A. The simple fit gives rise to a centroid mass of $M_8^{(\infty)} = 0.22354(17)(20)$ t.l.u $= 1255.1(1.0)(1.1)(8.2)$ MeV. Also shown in fig. 13 are the predictions of both $\mathrm{SU}(2)_L \otimes \mathrm{SU}(2)_R$ and $\mathrm{SU}(3)_L \otimes \mathrm{SU}(3)_R$ NLO HB$\chi$PT resulting from the same input parameters (not the fit parameters) as those used for the predictions of the individual baryon masses. In particular, the SU(3) relations between the decuplet-octet axial coupling constants, and between the octet-octet kaon and $\eta$ axial couplings, are employed. Given the overall general agreement between the leading predictions and the individual baryon masses, it is unsurprising that the $\mathrm{SU}(3)_L \otimes \mathrm{SU}(3)_R$ prediction for the centroid mass of the octet agrees reasonably well with the results of the Lattice QCD calculation.

#### *2. The $\Sigma$-$\Lambda$ Mass Splitting*

The mass difference between the $\Sigma$ and the $\Lambda$ vanishes in the limit of exact SU(3) symmetry. In Nature, the splitting is found to be $M_\Sigma - M_\Lambda \sim 74$ MeV, and consequently, at the pion mass of the Lattice QCD calculations, the calculated splitting is expected to be small. The results of the Lattice QCD calculation are shown in fig. 14, along with the results of a simple fit, of the form given in eq. (14), shown as the shaded regions. The result of the simple fit gives $(M_\Sigma - M_\Lambda)^{(\infty)} = 0.006598(48)(63)$ t.l.u $= 37.05(27)(35)(24)$ MeV, which is approximately half of its value at the physical quark masses. This is, in part, due to the strange quark mass used in the calculation being somewhat lighter than its value in Nature. The finite-volume contributions significantly suppress the mass splitting in smaller volumes.

The NLO expressions for the mass splitting do not describe the observed volume dependence well. While the full $\mathrm{SU}(3)_L \otimes \mathrm{SU}(3)_R$ NLO amplitude agrees in its sign with the volume dependence, the magnitude is significantly smaller than the results of the Lattice QCD calculations. It is clear that SU(3) breaking contributions that enter at higher orders in the chiral expansion play an important role in the volume dependence of the $\Sigma$-$\Lambda$ mass splitting.

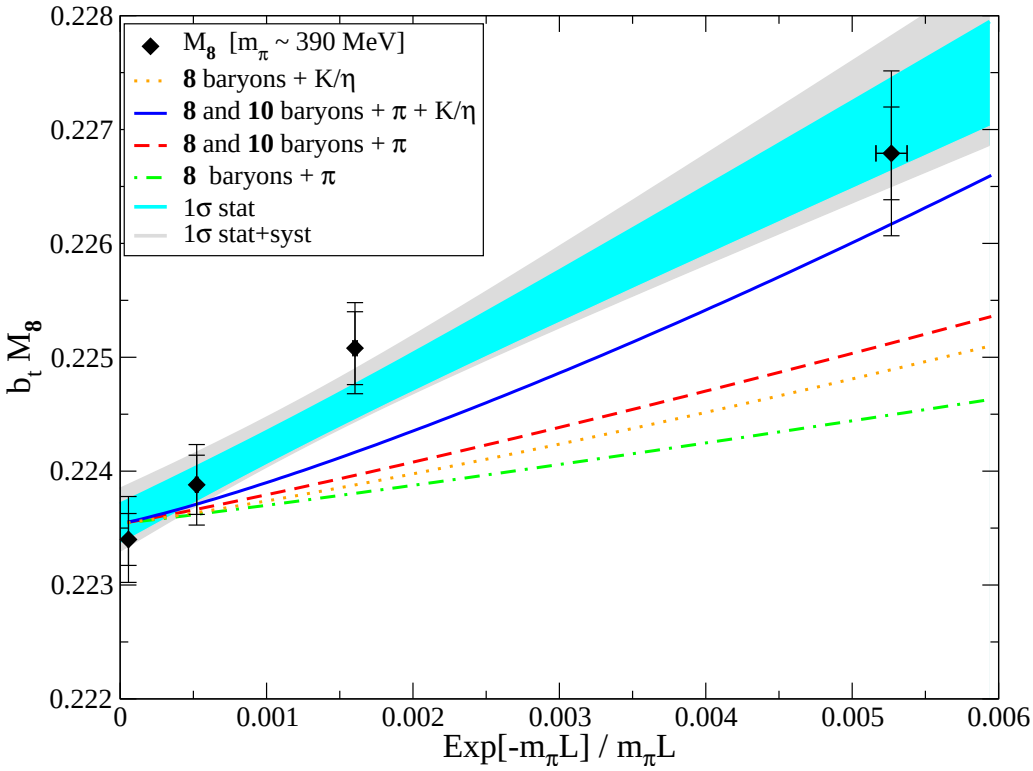


FIG. 13: The centroid of the baryon octet as a function of $e^{-m_\pi L}/(m_\pi L)$. The dark (light) grey shaded region corresponds to the $1\sigma$ statistical uncertainty (statistical and systematic uncertainties combined in quadrature) resulting from fitting the $m_\pi L = \infty$ value and the coefficient of $e^{-m_\pi L}/(m_\pi L)$. Using the value at $m_\pi L = \infty$, the dot-dashed curve (green) corresponds to the contribution from octet baryons and pions, the dotted curve (orange) corresponds to the contribution from octet baryons and kaons or an $\eta$, the dashed curve (red) corresponds to the contribution from octet and decuplet baryons and pions, and the solid curve (blue) corresponds to the contribution from octet and decuplet baryons and pions, kaons or an $\eta$.

### *3. The Gell-Mann–Okubo Mass Relation*

The GMO relation,

$$\text{GMO} \;=\; M_\Lambda \;+\; \frac{1}{3}M_\Sigma \;-\; \frac{2}{3}M_N \;-\; \frac{2}{3}M_\Xi \quad , \tag{24}$$

vanishes in the limit of exact SU(3) flavor symmetry, and also vanishes in the limit where the SU(3) breaking transforms as an **8** under SU(3) flavor symmetry. Consequently, it is a valuable probe of the structure of flavor symmetry breaking, being non-zero only for breaking that transform in the **27** irreducible representations of SU(3) [10]. The results of the Lattice QCD calculations are shown in fig. 15, along with the results of the simple fit, of the form given in eq. (14), shown as the shaded regions. The result of the simple fit gives

[10] Only the symmetric irreps in $\mathbf{8} \otimes \mathbf{8} = \mathbf{27} \oplus \mathbf{10} \oplus \overline{\mathbf{10}} \oplus \mathbf{8} \oplus \mathbf{8} \oplus \mathbf{1}$ are allowed, i.e. the **27**, **8**, and **1**. By construction the **8** and **1** do not contribute.

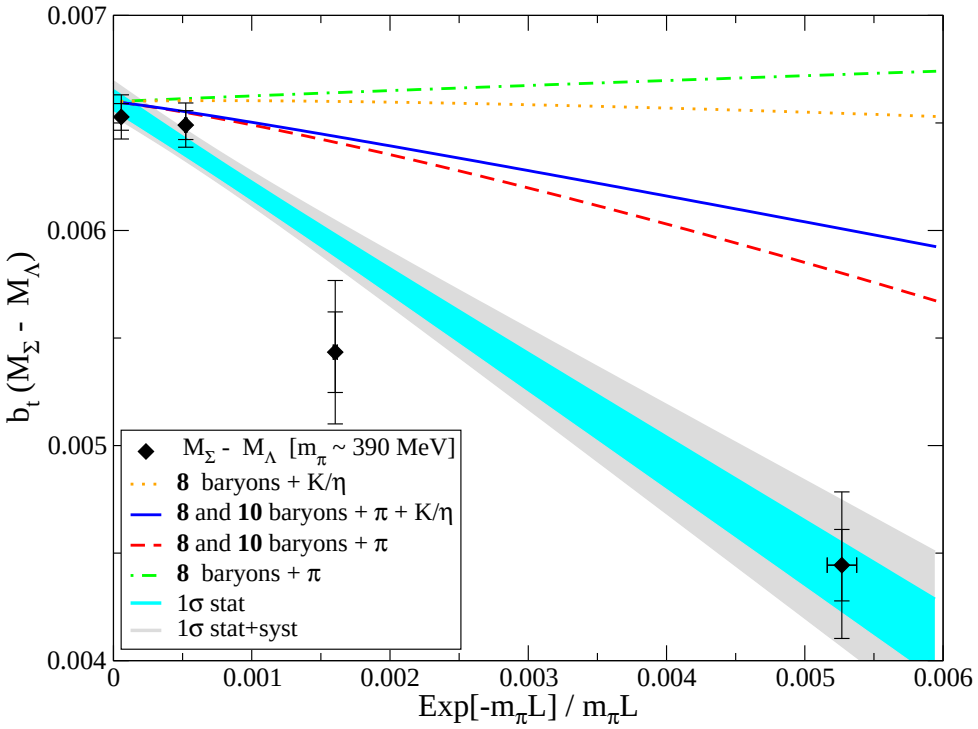


FIG. 14: The $\Sigma$-$\Lambda$ mass difference as a function of $e^{-m_\pi L}/(m_\pi L)$. The dark (light) grey shaded region corresponds to the $1\sigma$ statistical uncertainty (statistical and systematic uncertainties combined in quadrature) resulting from fitting $(M_\Sigma - M_\Lambda)^{(\infty)}$ and the coefficient of $e^{-m_\pi L}/(m_\pi L)$. Using this value of $(M_\Sigma - M_\Lambda)^{(\infty)}$, the dot-dashed curve (green) corresponds to the contribution from octet baryons and pions, the dotted curve (orange) corresponds to the contribution from octet baryons and kaons or an $\eta$, the dashed curve (red) corresponds to the contribution from octet and decuplet baryons and pions, and the solid curve (blue) corresponds to the contribution from octet and decuplet baryons and pions, kaons or an $\eta$.

$\text{GMO}^{(\infty)} = 3.49(25)(46) \times 10^{-4}$ t.l.u $= 1.96(14)(26)(01)$ MeV. Given the smallness of the GMO combination, it is no surprise that it has a large volume dependence, even changing sign between the $20^3 \times 128$ and the $24^3 \times 128$ lattice volumes.

As the GMO relation is sensitive only to the **27** SU(3) breaking, both the finite-volume and infinite-volume contributions are calculable in $\text{SU}(3)_L \otimes \text{SU}(3)_R$ HB$\chi$PT at one loop (which gives a finite result). It is straightforward to show that the infinite-volume value of the GMO relation is [19]

$$GMO^{(NLO)} = \frac{1}{24\pi f_\pi^2}\left[\left(\frac{2}{3}D^2 - 2F^2\right)\left(4m_K^3 - 3m_\eta^3 - m_\pi^3\right) - \frac{\mathcal{C}^2}{9\pi}\left(4F_K - 3F_\eta - F_\pi\right)\right], \quad (25)$$

where the function $F_c = F(m_c, \Delta, \mu)$ is

$$F(m,\Delta,\mu) = \left(m^2 - \Delta^2\right)\left(\sqrt{\Delta^2 - m^2}\log\left(\frac{\Delta - \sqrt{\Delta^2 - m^2 + i\epsilon}}{\Delta + \sqrt{\Delta^2 - m^2 + i\epsilon}}\right) - \Delta\log\left(\frac{m^2}{\mu^2}\right)\right) - \frac{1}{2}\Delta m^2 \log\left(\frac{m^2}{\mu^2}\right) \quad . \quad (26)$$

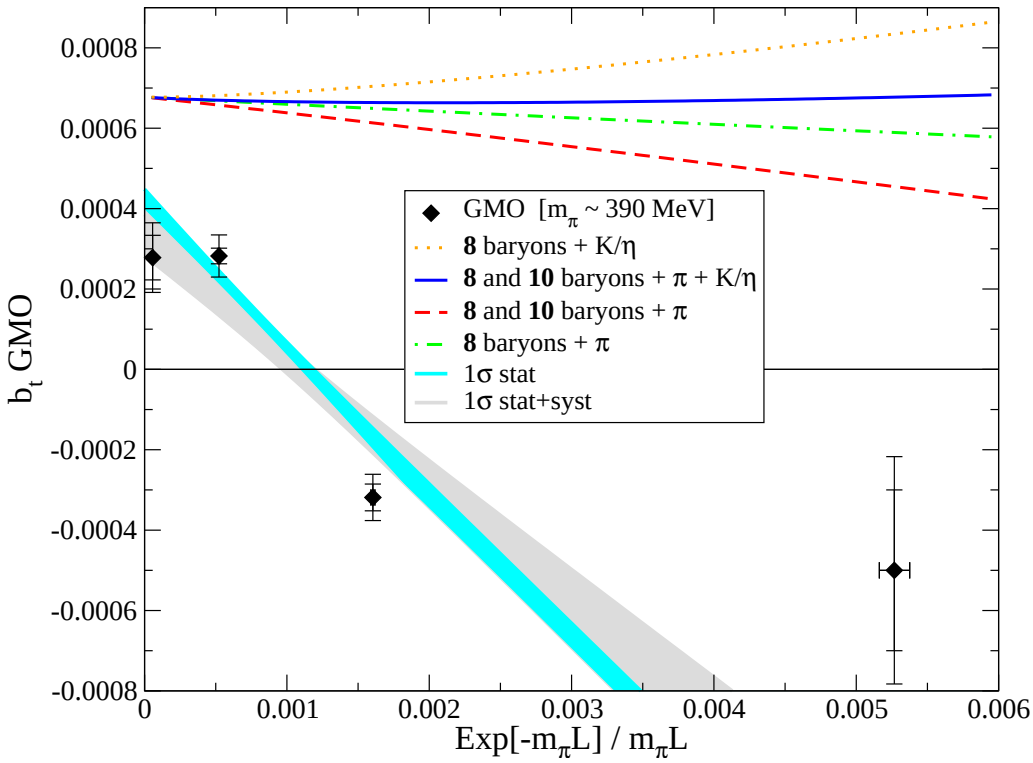


FIG. 15: The GMO relation as a function of $e^{-m_\pi L}/(m_\pi L)$. The dark (light) grey shaded region corresponds to the $1\sigma$ statistical uncertainty (statistical and systematic uncertainties combined in quadrature) resulting from fitting the $m_\pi L = \infty$ value and the coefficient of $e^{-m_\pi L}/(m_\pi L)$. The dot-dashed curve (green) corresponds to the contribution from octet baryons and pions, the dotted curve (orange) corresponds to the contribution from octet baryons and kaons or an $\eta$, the dashed curve (red) corresponds to the contribution from octet and decuplet baryons and pions, and the solid curve (blue) corresponds to the contribution from octet and decuplet baryons and pions, kaons or an $\eta$.

We have set $f_\pi = f_K = 150$ MeV in the GMO relation to eliminate formally higher-order contributions that depend upon the renormalization scale, $\mu$, from this expression. Inserting the values of the constants and parameters that we have used previously into eq. (26) gives a value of $\mathrm{GMO}^{(NLO)} \sim 6.8\times10^{-4}$ t.l.u., which is a factor of two greater than the extrapolation of the Lattice QCD results. This is not that surprising given the expected size of the higher-order contributions in the HB$\chi$PT expansion, as well as the fact that this quantity is anomalously small (suppressed beyond naive expectations based upon SU(3) symmetry alone due to a further suppression by $1/N_c^2$ in the large-$N_c$ limit of QCD [11]).

The NLO predictions of the volume dependence of the GMO relation in $\mathrm{SU}(2)_L \otimes \mathrm{SU}(2)_R$ and $\mathrm{SU}(3)_L \otimes \mathrm{SU}(3)_R$ HB$\chi$PT are shown in fig. 15. The contribution from the kaons and the $\eta$ are of opposite sign to that from the pion (as expected from their cancellation in the SU(3) limit), which gives rise to a small volume dependence, even on the scale of fig. 15.

[11] If $\epsilon \sim m_s - m_{u,d}$ denotes the SU(3) breaking parameter, then the GMO relation scales as $\sim \epsilon^{3/2}/N_c^2$ relative to the baryon masses; see, for example, eq. (25). For a review, see Ref. [47].

The predictions for the volume dependence of the GMO relation are in clear contradiction with the results of the Lattice QCD calculations. Clearly NLO HB$\chi$PT does not describe the higher-dimensional SU(3) breaking that provides the finite-volume dependence of the GMO relation, and we have found that this relation is particularly sensitive to the volume of the lattice.

The GMO relation was previously explored by some of the present authors [44, 48]. At approximately the same pion mass, and in the volume with $L \sim 2.5$ fm, the GMO relation was found to be positive and consistent with the loop-level expression given in eq. (26). This is in slight disagreement with the current determination; however, neither calculation extracts values in the continuum limit and the difference in this very small quantity may arise from the different discretizations and/or the somewhat different values of the strange-quark mass.

#### *4. The $R_4$ Mass Relation*

The $R_4$ relation, defined to be

$$R_4 \;=\; \frac{1}{6}\;\left(\; M_N \;+ M_\Lambda \;+\; M_\Xi \;-\; 3M_\Sigma \;\right) \quad , \tag{27}$$

vanishes in the limit of exact SU(3) flavor symmetry, and is formally dominated by a single insertion of the light-quark mass matrix in the infinite volume limit. This relation is of phenomenological interest because not only does it vanish in the limit of exact SU(3) flavor symmetry, but it also vanishes in the large-$N_c$ limit of QCD [47, 49, 50], scaling as $\sim \epsilon/N_c$ relative to the baryon masses ($\epsilon$ is defined in the footnote in subsection IV C 3). Recently, this relation, along with other relations among masses were examined with Lattice QCD calculations in work by Jenkins *et al.* [50] using domain-wall light-quark and strange-quark propagators generated on a number of ensembles of improved Kogut-Susskind dynamical quarks [51, 52]. The results of the present Lattice QCD calculations are shown in fig. 16, along with the results of the simple fit, of the form given in eq. (14), shown as the shaded regions. The result of the simple fit gives $R_4^{(\infty)} = -0.002757(27)(40)$ t.l.u $= -15.48(15)(22)(09)$ MeV, which is approximately half of its value at the physical quark masses, $R_4^{\rm expt} = -34.5$ MeV. The finite-volume contributions significantly suppress the mass splitting in smaller volumes.

The NLO expressions for $R_4$ do not describe the observed volume dependence well. While the full $\mathrm{SU}(3)_L \otimes \mathrm{SU}(3)_R$ NLO amplitude agrees in its sign with the volume dependence, the magnitude is significantly smaller than the results of the Lattice QCD calculations. SU(3) breaking contributions that enter beyond NLO in HB$\chi$PT play an important role in the $R_4$ mass relation.

## V. THE VOLUME DEPENDENCE OF THE MESON MASSES

It is also interesting to explore the volume dependence of the meson masses, specifically that of the pion and the kaon. There has been significantly more theoretical and numerical exploration of the meson masses and how they depend upon the volume of the lattices used in Lattice QCD calculations. An overview of the theoretical status of such finite-volume contributions can be found in Ref. [53].

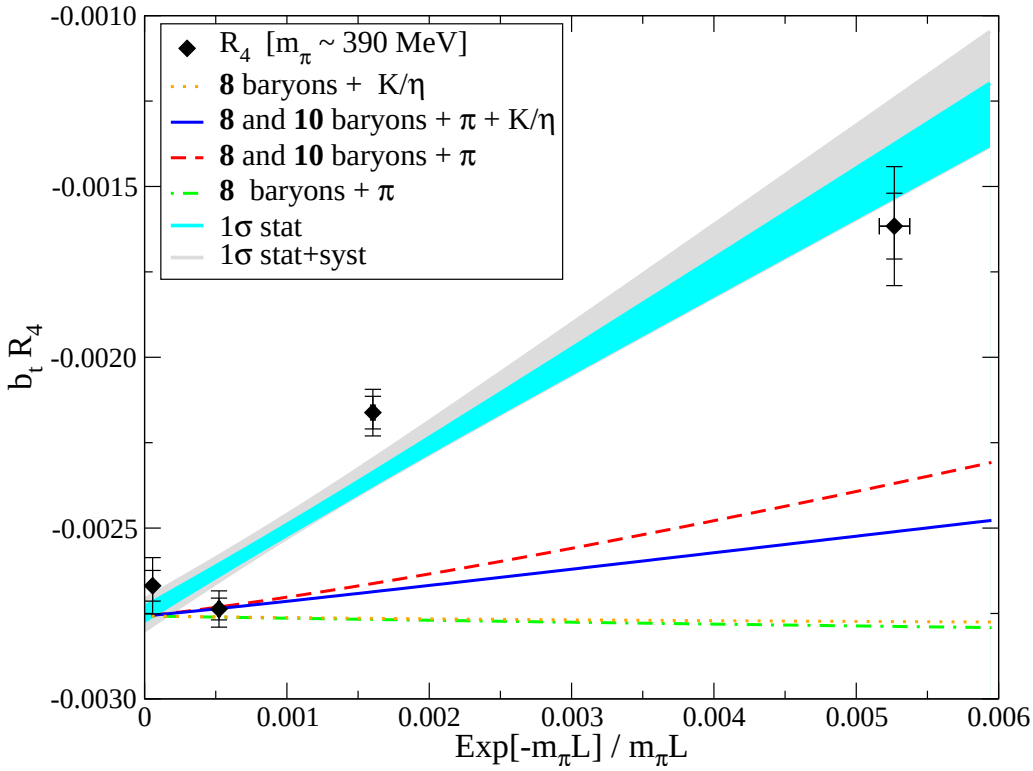


FIG. 16: The $R_4$ mass relation as a function of $e^{-m_\pi L}/(m_\pi L)$. The dark (light) grey shaded region corresponds to the $1\sigma$ statistical uncertainty (statistical and systematic uncertainties combined in quadrature) resulting from fitting the $m_\pi L = \infty$ value and the coefficient of $e^{-m_\pi L}/(m_\pi L)$. The dot-dashed curve (green) corresponds to the contribution from octet baryons and pions, the dotted curve (orange) corresponds to the contribution from octet baryons and kaons or an $\eta$, the dashed curve (red) corresponds to the contribution from octet and decuplet baryons and pions, and the solid curve (blue) corresponds to the contribution from octet and decuplet baryons and pions, kaons or an $\eta$.

The results of the present Lattice QCD calculations of the meson masses in the four different lattice volumes are given in table IV and the EMP's are shown in fig. 17 and fig. 18.

TABLE IV: Meson masses from the Lattice QCD calculations in the four lattice volumes.

| $L^3 \times T$ | $16^3 \times 128$ | $20^3 \times 128$ | $24^3 \times 128$ | $32^3 \times 256$ |
|---|---|---|---|---|
| $m_\pi$ (t.l.u.) | 0.06943(36)(0) | 0.06936(12)(0) | 0.06903(19)(0) | 0.069060(66)(81) |
| $m_K$ (t.l.u.) | 0.09722(26)(0) | 0.09702(10)(03) | 0.09684(15)(01) | 0.096984(78)(60) |

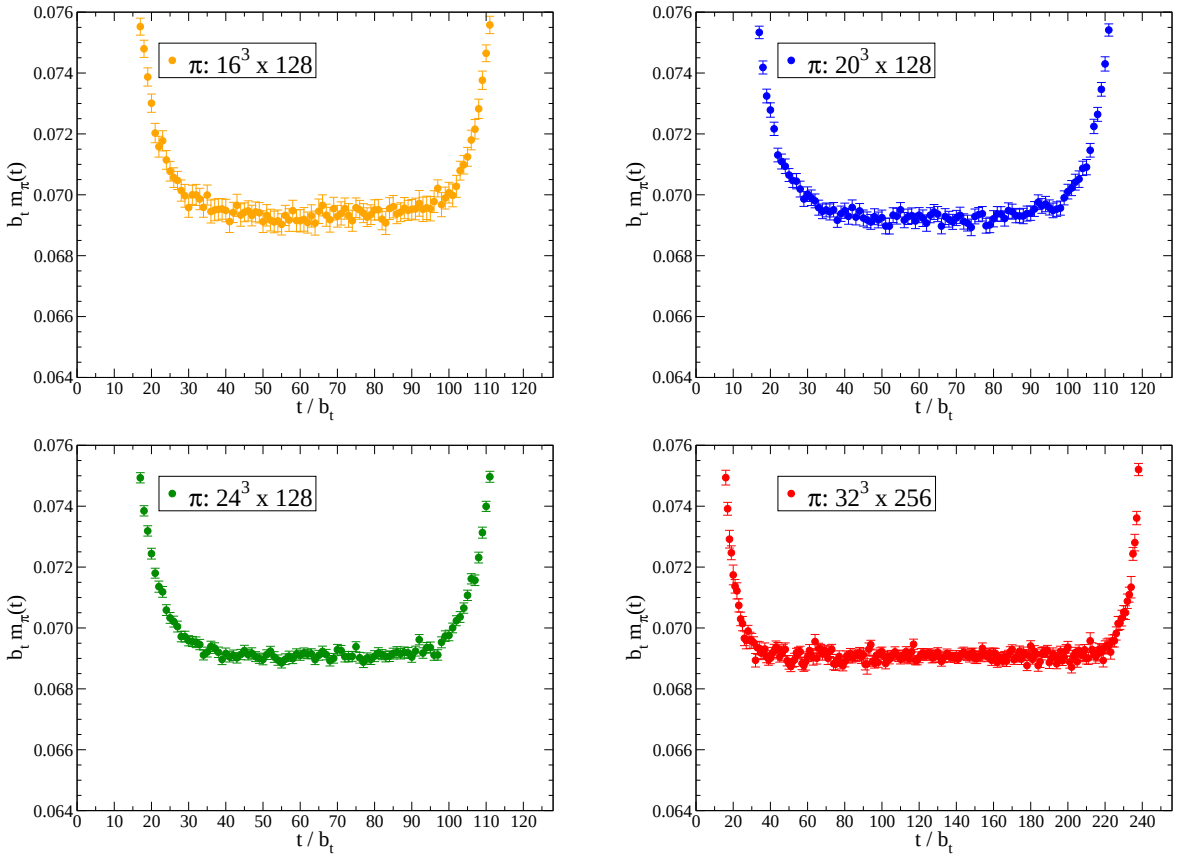


FIG. 17: The pion EMP's determined on the four lattice ensembles used in this work. Note that the y-axis scale is the same in all four panels.

### A. The Pion Mass

The finite-volume contribution to the mass of the pion in $\mathrm{SU}(2)_L \otimes \mathrm{SU}(2)_R$ $\chi$PT is given by [11]

$$m_\pi(L) - m_\pi(\infty) = \frac{3m_\pi^3}{4\pi^2 f_\pi^2}\frac{1}{m_\pi L}\left[K_1(m_\pi L) + \sqrt{2}K_1(\sqrt{2}m_\pi L) + \frac{4}{3\sqrt{3}}K_1(\sqrt{3}m_\pi L) + \ldots\right] \quad (28)$$

where $K_1(x)$ is the modified Bessel function. The meson masses have different overall volume scaling to the baryons, due to the absence of a three-meson vertex. As $K_1(z) \to e^{-z}/\sqrt{z}$, the results of the Lattice QCD calculations are shown in fig. 19 as a function of $e^{-m_\pi L}/(m_\pi L)^{3/2}$ rather than $e^{-m_\pi L}/(m_\pi L)$ as was used for the baryons. Consequently, the naive fit that we perform to the meson masses is of the form

$$m_M^{(V)}(m_\pi L) \;=\; m_M^{(\infty)} \;+\; c_M^{(V)}\;\frac{e^{-m_\pi\ L}}{(m_\pi L)^{3/2}} \quad . \quad (29)$$

With the current precision of the Lattice QCD calculation, we cannot distinguish between the fit forms of $e^{-m_\pi L}/(m_\pi L)$ and $e^{-m_\pi L}/(m_\pi L)^{3/2}$ with statistical significance. The fit parameters are $m_\pi^{(\infty)} = 0.069073(63)(62)$ t.l.u. $= 387.8(0.4)(0.4)(2.5)$ MeV and $c_\pi^{(V)} = 0.23(12)(07)$ t.l.u. $= (1.30(65)(39)(01)) \times 10^3$ MeV.

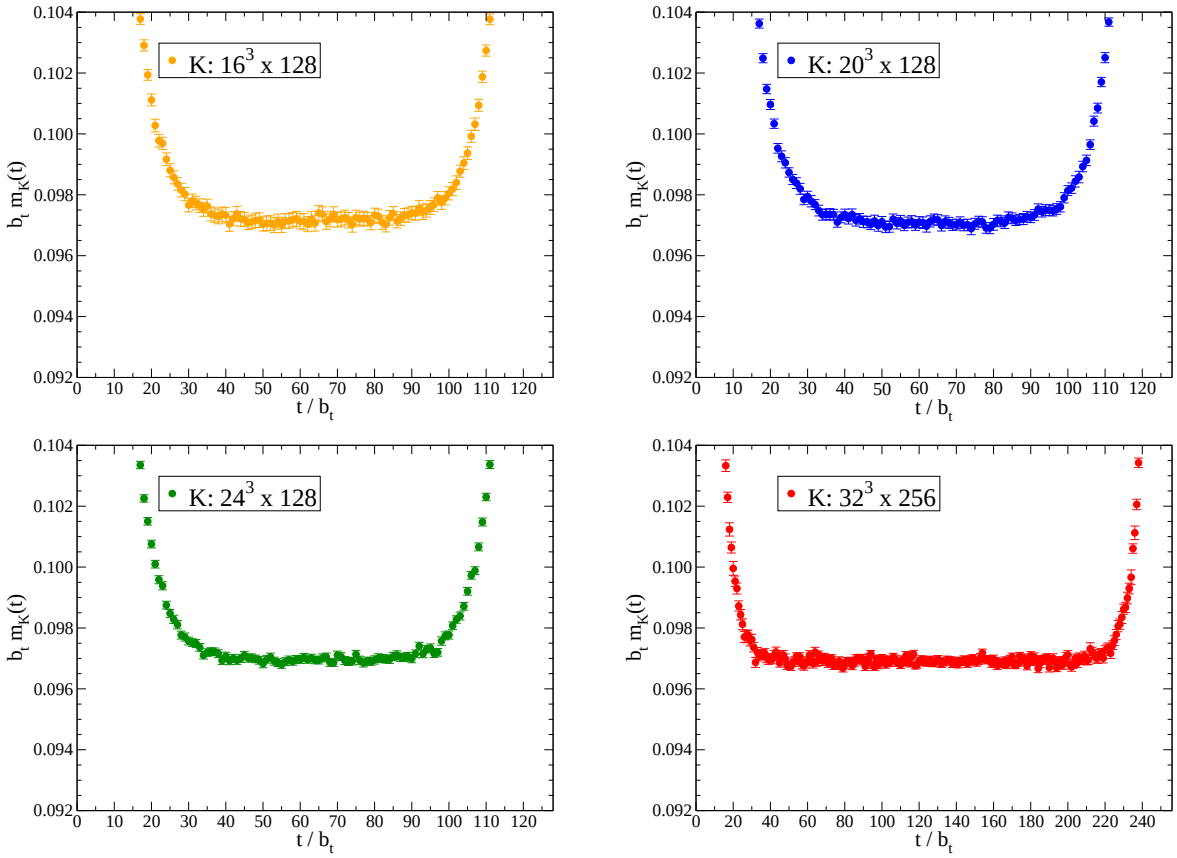


FIG. 18: The kaon EMP's determined on the four lattice ensembles used in this work. Note that the y-axis scale is the same in all four panels.

At NLO in $\mathrm{SU}(3)_L \otimes \mathrm{SU}(3)_R$ $\chi$PT, the finite-volume corrections to the pion mass are given by [53]

$$\delta m_\pi = \frac{3m_\pi^3}{4\pi^2 f_\pi^2}\frac{1}{m_\pi L}\left[K_1(m_\pi L) + \sqrt{2}K_1(\sqrt{2}m_\pi L) + \frac{4}{3\sqrt{3}}K_1(\sqrt{3}m_\pi L) + ...\right] - \frac{m_\pi m_\eta^2}{4\pi^2 f_\eta^2}\frac{1}{m_\eta L}\left[K_1(m_\eta L) + \sqrt{2}K_1(\sqrt{2}m_\eta L) + \frac{4}{3\sqrt{3}}K_1(\sqrt{3}m_\eta L) + ...\right] \quad (30)$$

Using the value of $m_\pi^{(\infty)}$ found in the fit to the form in eq. (29), the predicted volume dependence is shown in fig. 19 as the solid ( $\mathrm{SU}(3)_L \otimes \mathrm{SU}(3)_R$) and dashed curves ( $\mathrm{SU}(2)_L \otimes \mathrm{SU}(2)_R$). The volume dependence that is found in the Lattice QCD calculations agrees with the expectations of NLO $\chi$PT, and is significantly smaller than that of the baryon masses.

### B. The Kaon Mass

The formalism describing the volume dependence of the kaon mass is analogous to that of the pion. The NLO calculation in $\mathrm{SU}(3)_L \otimes \mathrm{SU}(3)_R$ $\chi$PT gives [53]

$$\delta m_K = \frac{m_K m_\eta^2}{2\pi^2 f_\eta^2}\frac{1}{m_\eta L}\left[K_1(m_\eta L) + \sqrt{2}K_1(\sqrt{2}m_\eta L) + \frac{4}{3\sqrt{3}}K_1(\sqrt{3}m_\eta L) + ...\right] \quad (31)$$

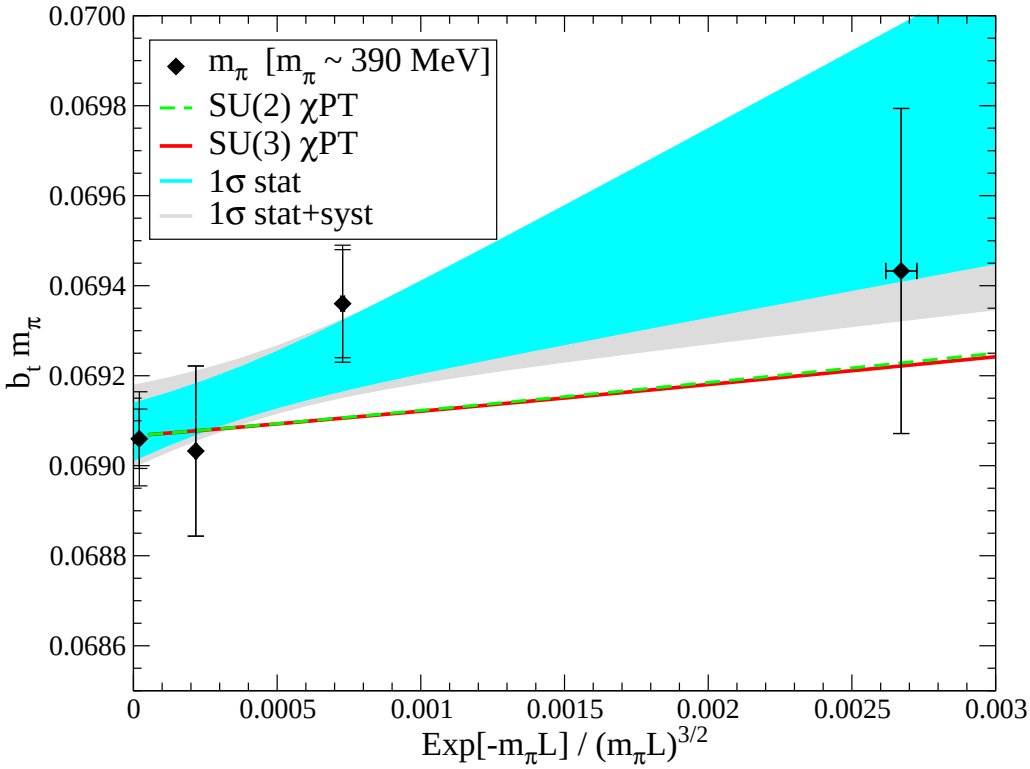


FIG. 19: The mass of the pion as a function of $e^{-m_\pi L}/(m_\pi L)^{3/2}$. The points and associated uncertainties (blue) are the results of the Lattice QCD calculations, as given in table IV. The dark (light) shaded region corresponds to the $1\sigma$ statistical uncertainty (statistical and systematic uncertainties combined in quadrature) associated with a fit of the form given in eq. (29). The solid (red) curve corresponds to the prediction of NLO $\mathrm{SU}(3)_L \otimes \mathrm{SU}(3)_R$ $\chi$PT, while the dashed (green) curve corresponds to the prediction of NLO $\mathrm{SU}(2)_L \otimes \mathrm{SU}(2)_R$ $\chi$PT using the value of $m_\pi^{(\infty)}$ found in the fit.

The results of the Lattice QCD calculation, given in table IV, are shown in fig. 20, along with a fit to the form given in eq. (29). The resulting fit values are $m_K^{(\infty)} = 0.096953(68)(39)$ t.l.u. $= 544.4(0.4)(0.2)(3.5)$ MeV and $c_K^{(V)} = 0.087(93)(44)$ t.l.u. $= (4.9(5.2)(2.5)(0.0)) \times 10^2$ MeV. The volume dependence of the kaon is found to be very small, much smaller than that of the baryons, and is consistent with the absence of pion loop contributions.

## VI. CONCLUSIONS

We have performed precise Lattice QCD calculations of the low-lying hadron masses at a pion mass of $m_\pi \sim 390$ MeV in four ensembles of anisotropic clover gauge-field configurations with a spatial lattice spacing of $b_s \sim 0.123$ fm, an anisotropy of $\xi = 3.5$ and cubic spatial lattice volumes with extent $L \sim 2.0, 2.5, 3.0$ and 3.9 fm. These calculations have allowed for a detailed exploration of the volume dependence of the octet baryon masses and of the pion and the kaon masses.

Our main conclusions are as follows:

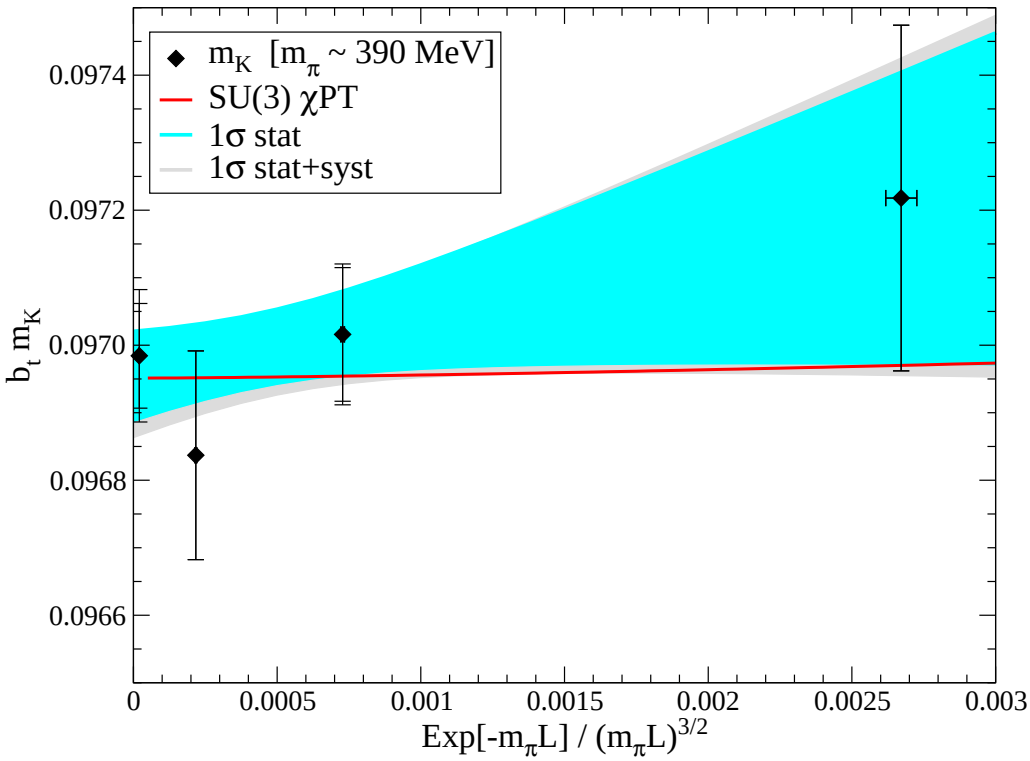


FIG. 20: The mass of the kaon as a function of $e^{-m_\pi L}/(m_\pi L)^{3/2}$. The points and associated uncertainties (blue) are the results of the Lattice QCD calculations, as given in table IV. The dark (light) shaded region corresponds to the $1\sigma$ statistical uncertainty (statistical and systematic uncertainties combined in quadrature) associated with a fit of the form given in eq. (29). The solid (red) curve corresponds to the prediction of NLO $\mathrm{SU}(3)_L \otimes \mathrm{SU}(3)_R$ $\chi$PT.

- In order to calculate individual baryon masses with percent-level precision ($\pm 10$ MeV), it is sufficient to work in volumes with $m_\pi L \gtrsim 4.3$ for $m_\pi \sim 390$ MeV, and NLO HB$\chi$PT indicates that somewhat smaller values of $m_\pi L$ may be sufficient at lighter pion masses.

- The expectations of NLO $\mathrm{SU}(3)_L \otimes \mathrm{SU}(3)_R$ HB$\chi$PT (with the meson decay constants evaluated at the appropriate meson mass) are found to qualitatively reproduce the lattice results for the volume dependence of all of the baryon and meson masses. The NLO $\mathrm{SU}(3)_L \otimes \mathrm{SU}(3)_R$ predictions are sufficiently accurate to allow for meaningful extrapolations to lighter pion masses to be made, where the volume dependences are expected to be significantly smaller. In the context of determinations of two-body interactions, this feature allows for gauge-field configurations with somewhat (logarithmically) smaller values of $m_\pi L$ to be used for the calculation of the interactions between baryons while keeping the exponential corrections to the Lüscher eigenvalue relation from single hadron masses negligibly small. A Lattice QCD calculation at the physical pion mass and in a volume with $m_\pi L = 5.8$ is predicted to generate finite-volume corrections to the nucleon mass of $\delta M_N \sim 100$ keV, smaller than the typical nuclear excitation energies found in light nuclei.

- The contributions from kaon and $\eta$ loops to the volume dependence of the nucleon mass

are small in $\mathrm{SU}(3)_L \otimes \mathrm{SU}(3)_R$ HB$\chi$PT, and therefore a relatively stable determination of $|g_{\Delta N\pi}|/g_A$ has been found, which can be systematically improved by working at higher orders in HB$\chi$PT. Given the size of the finite-volume contributions to the masses of the hyperons from kaon and $\eta$ loops, we have not made significant determinations of the hyperon axial coupling constants in the two-flavor chiral expansion. However, Lattice QCD calculations at lighter pion masses should enable a determination of these couplings.

- The GMO relation is found to exhibit substantial volume dependence, with the relation changing sign at $m_\pi L \sim 5.2$ with $m_\pi \sim 390$ MeV. Perhaps this should not be surprising given the delicate cancellations that occur between the baryon masses to leave a quantity that depends only upon SU(3)-breaking in the **27**-dimensional irreducible representation and vanishes in the large-$N_c$ limit as $1/N_c^2$ compared to the individual baryon masses.

We thank G. Colangelo for valuable conversations, K. Roche for computing resources at ORNL NCCS and R. Edwards and B. Joo for developing QDP++, Chroma [54] and production. We acknowledge computational support from the USQCD SciDAC project, NERSC (Office of Science of the DOE, Grant No. DE-AC02-05CH11231), the UW HYAK facility, Centro Nacional de Supercomputación (Barcelona, Spain), LLNL, the Argonne Leadership Computing Facility at Argonne National Laboratory (Office of Science of the DOE, under contract No. DE-AC02-06CH11357), and the NSF through Teragrid resources provided by TACC and NICS under Grant No. TG-MCA06N025. SRB was supported in part by the NSF CAREER Grant No. PHY-0645570. The Albert Einstein Center for Fundamental Physics is supported by the Innovations- und Kooperationsprojekt C-13 of the Schweizerische Universitätskonferenz SUK/CRUS. The work of EC and AP is supported by the contract FIS2008-01661 from MEC (Spain) and FEDER. AP acknowledges support from the RTN Flavianet MRTN-CT-2006-035482 (EU). BJ was also supported by DOE Grants, No. DE-FC02-06ER41440 and No. DE-FC02-06ER41449 (SciDAC USQCD). H-WL and MJS were supported in part by the DOE Grant No. DE-FG03-97ER4014. WD and KO were supported in part by DOE Grants No. DE-AC05-06OR23177 (JSA) and No. DE-FG02-04ER41302. WD was also supported by DOE OJI Grant No. DE-SC0001784 and Jeffress Memorial Trust, Grant No. J-968. KO was also supported in part by NSF Grant No. CCF-0728915 and DOE OJI Grant No. DE-FG02-07ER41527. AT was supported by NSF Grant No. PHY-0555234 and DOE Grant No. DE-FC02-06ER41443. The work of TL was performed under the auspices of the U.S. Department of Energy by LLNL under Contract No. DE-AC52-07NA27344 and the UNEDF SciDAC Grant No. DE-FC02-07ER41457. The work of AWL was supported in part by the Director, Office of Energy Research, Office of High Energy and Nuclear Physics, Divisions of Nuclear Physics, of the U.S. DOE under Contract No. DE-AC02-05CH11231.

[1] H. W. Hamber, E. Marinari, G. Parisi and C. Rebbi, Nucl. Phys. B **225**, 475 (1983).
[2] M. Lüscher, Commun. Math. Phys. **105**, 153 (1986).
[3] M. Lüscher, Nucl. Phys. B **354**, 531 (1991).

[4] P. F. Bedaque, I. Sato and A. Walker-Loud, Phys. Rev. D **73**, 074501 (2006) [arXiv:hep-lat/0601033].
[5] I. Sato, P. F. Bedaque, Phys. Rev. **D76**, 034502 (2007). [hep-lat/0702021 [HEP-LAT]].
[6] S. R. Beane *et al.* [NPLQCD Collaboration], *To appear in Phys. Rev. Lett.*, arXiv:1012.3812 [hep-lat].
[7] S. R. Beane *et al.*, Phys. Rev. D **79**, 114502 (2009) [arXiv:0903.2990 [hep-lat]].
[8] S. R. Beane *et al.*, Phys. Rev. D **80**, 074501 (2009) [arXiv:0905.0466 [hep-lat]].
[9] S. R. Beane *et al.* [NPLQCD Collaboration], Phys. Rev. D **81** (2010) 054505 [arXiv:0912.4243 [hep-lat]].
[10] A. Ali Khan *et al.* [ QCDSF-UKQCD Collaboration ], Nucl. Phys. **B689**, 175-194 (2004). [hep-lat/0312030].
[11] J. Gasser, H. Leutwyler, Phys. Lett. **B184**, 83 (1987).
[12] J. Gasser, H. Leutwyler, Phys. Lett. **B188**, 477 (1987).
[13] J. Gasser, H. Leutwyler, Nucl. Phys. **B307**, 763 (1988).
[14] M. Lüscher, Commun. Math. Phys. **104**, 177 (1986).
[15] G. Colangelo, A. Fuhrer and C. Haefeli, Nucl. Phys. Proc. Suppl. **153**, 41 (2006) [arXiv:hep-lat/0512002].
[16] G. Colangelo, A. Fuhrer, S. Lanz, Phys. Rev. **D82**, 034506 (2010). [arXiv:1005.1485 [hep-lat]].
[17] S. R. Beane, Phys. Rev. D **70**, 034507 (2004) [arXiv:hep-lat/0403015].
[18] B. C. Tiburzi, A. Walker-Loud, Phys. Lett. **B669**, 246-253 (2008). [arXiv:0808.0482 [nucl-th]].
[19] E. Jenkins, Nucl. Phys. B **368**, 190 (1992).
[20] J. J. Dudek, R. G. Edwards, M. J. Peardon, D. G. Richards and C. E. Thomas, Phys. Rev. Lett. **103**, 262001 (2009) [arXiv:0909.0200 [hep-ph]].
[21] J. M. Bulava *et al.*, Phys. Rev. D **79**, 034505 (2009) [arXiv:0901.0027 [hep-lat]].
[22] H. W. Lin *et al.* [Hadron Spectrum Collaboration], Phys. Rev. D **79**, 034502 (2009) [arXiv:0810.3588 [hep-lat]].
[23] R. G. Edwards, B. Joo and H. W. Lin, Phys. Rev. D **78**, 054501 (2008) [arXiv:0803.3960 [hep-lat]].
[24] M. Okamoto *et al.* [CP-PACS Collaboration], Phys. Rev. D **65**, 094508 (2002) [arXiv:hep-lat/0112020].
[25] P. Chen, Phys. Rev. D **64**, 034509 (2001) [arXiv:hep-lat/0006019].
[26] C. Morningstar and M. J. Peardon, Phys. Rev. D **69**, 054501 (2004) [arXiv:hep-lat/0311018].
[27] S. R. Beane, W. Detmold, K. Orginos, M. J. Savage, Prog. Part. Nucl. Phys. **66**, 1, (2011) [arXiv:1004.2935 [hep-lat]].
[28] R. G. Edwards *et al.* [LHPC Collaboration], Phys. Rev. Lett. **96**, 052001 (2006) [arXiv:hep-lat/0510062].
[29] T. Yamazaki *et al.* [RBC+UKQCD Collaboration], Phys. Rev. Lett. **100**, 171602 (2008) [arXiv:0801.4016 [hep-lat]].
[30] M. Gockeler *et al.* [QCDSF/UKQCD Collaboration], PoS **LATTICE2010**, 163 (2010) [arXiv:1102.3407 [hep-lat]].
[31] C. Alexandrou *et al.* [ETM Collaboration], Phys. Rev. D **83**, 045010 (2011) [arXiv:1012.0857 [hep-lat]].
[32] H. W. Lin and K. Orginos, Phys. Rev. D **79**, 034507 (2009) [arXiv:0712.1214 [hep-lat]].
[33] C. Allton *et al.* [RBC-UKQCD Collaboration], Phys. Rev. D **78**, 114509 (2008) [arXiv:0804.0473 [hep-lat]].
[34] P. Dimopoulos, R. Frezotti, G. Herdoiza, K. Jansen, C. Michael and C. Urbach [ETM Collab-

oration], PoS E **FT09**, 039 (2009) [arXiv:0912.5197 [hep-ph]].
[35] A. Bazavov *et al.* [The MILC Collaboration], PoS **LAT2009**, 077 (2009) [arXiv:0911.0472 [hep-lat]].
[36] S. R. Beane, P. F. Bedaque, K. Orginos and M. J. Savage, Phys. Rev. D **75**, 094501 (2007) [arXiv:hep-lat/0606023].
[37] R. Flores-Mendieta, E. E. Jenkins and A. V. Manohar, Phys. Rev. D **58**, 094028 (1998) [arXiv:hep-ph/9805416].
[38] T. R. Hemmert, B. R. Holstein and N. C. Mukhopadhyay, Phys. Rev. D **51**, 158 (1995) [arXiv:hep-ph/9409323].
[39] C. Alexandrou, G. Koutsou, T. Leontiou, J. W. Negele and A. Tsapalis, Phys. Rev. D **76**, 094511 (2007) [Erratum-ibid. D **80**, 099901 (2009)] [arXiv:0706.3011 [hep-lat]].
[40] C. Alexandrou, G. Koutsou, J. W. Negele, Y. Proestos and A. Tsapalis, Phys. Rev. D **83**, 014501 (2011) [arXiv:1011.3233 [hep-lat]].
[41] A. Fuhrer, Ph.D. Thesis, Universität Bern, 2004.
[42] G. Colangelo, C. Haefeli, Nucl. Phys. **B744**, 14-33 (2006). [hep-lat/0602017].
[43] M. J. Savage and J. Walden, Phys. Rev. D **55**, 5376 (1997) [arXiv:hep-ph/9611210].
[44] A. Walker-Loud, H. -W. Lin, D. G. Richards, R. G. Edwards, M. Engelhardt, G. T. Fleming, P. .Hagler, B. Musch *et al.*, Phys. Rev. **D79**, 054502 (2009). [arXiv:0806.4549 [hep-lat]].
[45] K. -I. Ishikawa *et al.* [ PACS-CS Collaboration ], Phys. Rev. **D80**, 054502 (2009). [arXiv:0905.0962 [hep-lat]].
[46] A. Torok, S. R. Beane, W. Detmold, T. C. Luu, K. Orginos, A. Parreno, M. J. Savage, A. Walker-Loud, Phys. Rev. **D81**, 074506 (2010). [arXiv:0907.1913 [hep-lat]].
[47] A. V. Manohar, arXiv:hep-ph/9802419.
[48] S. R. Beane, K. Orginos and M. J. Savage, Phys. Lett. B **654**, 20 (2007) [arXiv:hep-lat/0604013].
[49] E. E. Jenkins and R. F. Lebed, Phys. Rev. D **52**, 282 (1995) [arXiv:hep-ph/9502227].
[50] E. E. Jenkins, A. V. Manohar, J. W. Negele and A. Walker-Loud, Phys. Rev. D **81**, 014502 (2010) [arXiv:0907.0529 [hep-lat]].
[51] K. Orginos *et al.* [ MILC Collaboration ], Phys. Rev. **D60**, 054503 (1999). [hep-lat/9903032].
[52] C. W. Bernard, T. Burch, K. Orginos, D. Toussaint, T. A. DeGrand, C. E. Detar, S. Datta, S. A. Gottlieb *et al.*, Phys. Rev. **D64**, 054506 (2001). [hep-lat/0104002].
[53] G. Colangelo, S. Dürr and C. Haefeli, Nucl. Phys. B **721**, 136 (2005) [arXiv:hep-lat/0503014].
[54] R. G. Edwards and B. Joo, Nucl. Phys. Proc. Suppl. **140** (2005) 832.